

# Towards better diagnosis and treatment of thrombotic thrombocytopenic purpura

**Aurélie DEWAELE**

Supervisor: Prof. dr. Karen Vanhoorelbeke

Mentor: *Charlotte Dekimpe*

Thesis presented in  
fulfillment of the requirements  
for the degree of Master of Science  
in de biochemie en de biotechnologie

Academic year 2018-2019

---

© Copyright by KU Leuven

Without written permission of the promotors and the authors it is forbidden to reproduce or adapt in any form or by any means any part of this publication. Requests for obtaining the right to reproduce or utilize parts of this publication should be addressed to KU Leuven, Faculteit Wetenschappen, Geel Huis, Kasteelpark Arenberg 11 bus 2100, 3001 Leuven (Heverlee), Telephone +32 16 32 14 01.

A written permission of the promotor is also required to use the methods, products, schematics and programs described in this work for industrial or commercial use, and for submitting this publication in scientific contests.

# Acknowledgement

Eerst en vooral, wil ik graag mijn promotor Prof. dr. Karen Vanhoorelbeke bedanken om me de kans te bieden mijn master af te ronden in het Labo voor Trombose Onderzoek.

Daarnaast wil ik mijn mentor Charlotte Dekimpe bedanken om me de afgelopen maanden te begeleiden. Charlotte, ik heb enorm veel van jou bijgeleerd daar is geen twijfel over mogelijk, maar ik wil jou vooral bedanken voor je geduld en je motiverende woorden. Bedankt, om me dit jaar onder je vleugels te nemen!

Ik wil Inge en Aline bedanken omdat ze, ondanks hun vele werk, altijd klaarstonden om mijn vragen te beantwoorden en mij de trucjes van het vak te leren. Graag wil ik ook Giles Vermeire bedanken voor zijn hulp bij het *in vitro* experiment.

To the rest of my (temporary) colleagues in the lab: Thank you for creating such an amazing working atmosphere. You were always willing to help and listen and for that I am extremely grateful. But most off all, a big thank you for making me laugh so much! Hé, Senna, ti waar hé! Thank you, Kim, for welcoming me with all your lovely pumpkin spiced baking. Tim, dankjewel voor je vriendelijke “Goeiemorgen, Aurélie” iedere morgen. Dat doet een mens meer deugd dan je beseft! And Cristiano, DO NOT, I repeat, DO NOT get fired because of your stupid jokes, please... Katleen, jou wil ik nog even extra bedanken voor al je hulp met de muisjes en om me altijd gerust te stellen. Daarnaast wil ik jullie allemaal heel veel succes wensen met jullie verdere toekomst en carrière!

Verder wil ik graag mijn vrienden van de Kulak bedanken: Dankjewel voor die mooie en hilarische momenten, dankjewel voor jullie steun tijdens de wat lasterige momenten, of om het in Jana haar woorden te zeggen: dikke vorte lovia's!

Jodie, Joke, Fleur, Elke, Laura, Liselotte, Irene, Saskia, Jasmien en Gwen, ook jullie verdienen allemaal een speciale vermelding. Jullie vriendschap doorheen deze vijf jaar en alle jaren voorheen betekent zoveel voor mij: merci voor alle pep talks, alle schouderklopjes, alle berichtjes maar ook alle etentjes, alle uitstapjes en al die keren dat jullie mijn gedachten hebben verzet op iets helemaal anders dan “school”.

Ten slotte wil ik ook nog mijn mama, papa, zus, mamie en papie bedanken, zonder jullie zou dit nooit gelukt zijn! Jullie steun is mijn grootste steun, en daarvoor uit de grond van mijn hart: dankjewel.

# Summary

Thrombotic thrombocytopenic purpura (TTP) is a rare and life-threatening disease caused by a deficiency in ADAMTS13. An acute TTP episode is a medical emergency and when TTP diagnosis is suspected, treatment should be initiated immediately. However, the complexity of TTP diagnosis and the time it takes to provide ADAMTS13 data leads to delays in TTP diagnosis and misdiagnosis of TTP patients. Furthermore, the mortality rate of TTP remains 10-20% and 40% of the patients that survive the initial TTP episode experience a relapse. Thus, both diagnosis and treatment remain a stumbling block for TTP management. In order to aid this dual challenge, this thesis focusses on three ADAMTS13 markers important for diagnosis and prognosis, namely ADAMTS13 activity, anti-ADAMTS13 autoantibodies and ADAMTS13 antigen, as well as developing a novel treatment strategy.

First of all, the VWF96 ADAMTS13 activity enzyme-linked immunosorbent assay (ELISA) was adapted for the use of citrated human plasma. Secondly, a cut-off value that discriminates between individuals with and without anti-ADAMTS13 autoantibodies was established as a part of the characterisation process of the in-house anti-ADAMTS13 autoantibody ELISA. Thirdly, ADAMTS13 antigen levels of a large cohort of samples, including 424 healthy donor and 19 patient plasma samples, were measured to characterise and validate the in-house ADAMTS13 antigen ELISA. Finally, a clinically relevant gene therapy approach using intramuscular electrotransfer to introduce plasmid DNA into muscle cells of *Adamts13*<sup>-/-</sup> mice is initiated. Therefore, full-length murine *ADAMTS13* cDNA was cloned into a plasmid containing the CAG promoter and *in vitro* expression was verified.

# Samenvatting

Trombotische trombocytopenische purpura (TTP) is een zeldzame en levensbedreigende ziekte veroorzaakt door een deficiëntie in ADAMTS13. Een acute TTP aanval is een medische noodsituatie en wanneer TTP vermoed wordt, moet onmiddellijk gestart worden met de bijpassende behandeling. TTP diagnose is echter complex en vaak zijn ADAMTS13 data niet onmiddellijk beschikbaar. Dit zorgt voor een verkeerde en vertraagde diagnose van TTP patiënten. Daarnaast blijft het sterftecijfer 10-20% en 40% van de patiënten die hun eerste TTP aanval overleven zullen hervallen. Dus zowel het diagnoseproces als de behandeling van TTP blijven een struikelblok en bijgevolg handelt deze thesis over beide aspecten, inclusief drie ADAMTS13 markers belangrijk voor diagnose en prognose, namelijk ADAMTS13 activiteit, anti-ADAMTS13 autoantilichamen en ADAMTS13 antigen, alsook een nieuwe behandelingsstrategie.

Ten eerste werd de VWF96 ADAMTS13 activiteit *enzyme-linked immunosorbent assay* (ELISA) aangepast voor gecitreerd humaan plasma. Ten tweede werd een *cut-off* waarde bepaald voor de *in-house* anti-ADAMTS13 autoantilichaam ELISA. Deze waarde discrimineert tussen individuen met en zonder anti-ADAMTS13 autoantilichamen. Ten derde werden ADAMTS13 antigen levels gemeten in een grote cohort van 443 plasmastalen, inclusief 424 gezonde donorstalen en 19 patiëntenstalen, om de *in-house* ADAMTS13 antigen ELISA te karakteriseren en te valideren. Ten slotte wordt een klinisch relevante gentherapie voorgesteld die gebruik maakt van intramusculaire elektrotransfer om plasmide DNA te introduceren in de spiercellen van *Adamts13<sup>-/-</sup>* muizen. Hiervoor, werd het muriene *ADAMTS13* cDNA gekloneerd in een plasmide die een CAG promotor bevat en werd *in vitro* expressie geverifieerd.

# List of Abbreviations

$\alpha$ IIb $\beta$ 3	integrin $\alpha$ IIb $\beta$ 3, also known as GPIIb/IIIa
aa	amino acids
ADA	anti-drug antibody
ADAMTS13	a disintegrin and metalloproteinase with a thrombospondin type 1 motif, member 13
ADAMTS13:Ag	ADAMTS13 antigen (level)
Bmp1	bone morphogenic protein 1
C	cysteine-rich domain of ADAMTS13
CAG promotor	cytomegalovirus immediate-early enhancer-chicken- $\beta$ -actin hybrid promotor
C1r/C1s	complement components C1r/C1s
CIC	circulating immune complexes or antigen-antibody complexes
CK	cystine knot domain of VWF, also called CTCK
CTCK	C-terminal cystine knot-like domain, also called CK
cTTP	congenital TTP
CUB	complement components C1r/C1s, Uegf and Bmp1
D	disintegrin-like domain
ELISA	enzyme-linked immunosorbent assay
ER	endoplasmic reticulum
Factor IIa	coagulation factor IIa or thrombin
FRET assay	fluorescence resonance energy transfer assay
FVIII	coagulation factor VIII
GPIb $\alpha$	platelet glycoprotein Iba
GPIIb/IIIa	platelet glycoprotein IIb/IIIa, also known as integrin $\alpha$ IIb $\beta$ 3
HBS	HEPES-buffered saline
HD	healthy donor
HELLP syndrome	haemolysis, elevated liver enzymes, low platelets syndrome
HIV	human immunodeficiency virus
HLA	human leukocyte antigen
HMW	high molecular weight
HRP	horseradish peroxidase
HSV	herpes simplex virus
HUS	haemolytic uraemic syndrome
Ig	immunoglobulin
IMW	intermediate molecular weight
iTTP	immune-mediated TTP

LDH	lactate dehydrogenase
LMW	low molecular weight
M	metalloprotease domain
mADAMTS13	murine ADAMTS13
MDCTS	N-terminal part of ADAMTS13
mut	mutated
NHP	normal human plasma
NMP	normal murine plasma
OD	optical density
ON	overnight
OPD	o-phenylenediamine dihydrochloride
P	propeptide
PBS	phosphate buffered saline
PCR	polymerase chain reaction
PEX	plasma exchange
rADAMTS13	recombinant ADAMTS13
RAG1	recombination activating gene 1
RGD	Arginine-Glycine-Aspartic acid
rhADAMTS13	recombinant human ADAMTS13
RT	room temperature
rVWF	recombinant VWF
S	spacer domain
SP	signal peptide
Stx	shigatoxin
T	thrombospondin type-1 repeat
TMA	thrombotic microangiopathy
TTP	thrombotic thrombocytopenic purpura
Uegf	urinary epidermal growth factor-related sea urchin protein
UL	ultra-large
VWF96	recombinant oligopeptide consisting of 96 aa residues of VWF A2 domain
WT	wild type
Y1605-M1606	Tyrosine1605 - Methionine1606, cleavage site for ADAMTS13 in VWF A2 domain

# Table of Contents

Acknowledgement .....	I
Summary .....	II
Samenvatting.....	III
List of Abbreviations .....	IV
<b>I Literature Review .....</b>	<b>1</b>
<b>1 Haemostasis .....</b>	<b>2</b>
<b>2 Von Willebrand factor .....</b>	<b>3</b>
1.2 Biosynthesis.....	4
2.2 Functional domains.....	6
2.2.1 A domain .....	6
2.2.2 D domains .....	7
2.2.3 C domains .....	7
2.2.4 CK domain .....	8
<b>3 ADAMTS13 .....</b>	<b>9</b>
3.1 Functional domains.....	9
3.1.1 Propeptide .....	10
3.1.2 Metalloprotease domain .....	10
3.1.3 Disintegrin-like domain .....	11
3.1.4 Cysteine-rich domain.....	12
3.1.5 Spacer domain .....	12
3.1.6 Thrombospondin Type-1 Repeats .....	12
3.1.7 CUB domains .....	12
3.2 Interaction of ADAMTS13 and VWF.....	13
<b>4 Thrombotic thrombocytopenic purpura .....</b>	<b>15</b>
4.1 Pathophysiology .....	15
4.2 Congenital and immune-mediated TTP.....	16
4.2.1 Congenital TTP .....	17

4.2.2 Immune-mediated TTP .....	17
4.3 Diagnosis .....	19
4.3.1 Clinical presentation .....	19
4.3.2 Differential diagnosis .....	20
4.3.3 Prognostic factors.....	21
4.4 Therapy .....	22
4.4.1 Congenital TTP .....	23
4.4.2 Immune-mediated TTP.....	23
4.4.3 Gene therapy.....	26
<b>5 Objectives .....</b>	<b>29</b>
<b>II Materials &amp; Methods .....</b>	<b>31</b>
<b>6 Diagnosis and prognosis.....</b>	<b>32</b>
6.1 Plasma Samples .....	32
6.2 Human ADAMTS13 activity ELISA.....	32
6.3 Human anti-ADAMTS13 autoantibody ELISA .....	34
6.4 Human ADAMTS13 antigen binding ELISA.....	35
<b>7 Gene therapy.....</b>	<b>37</b>
7.1 Construction of the pMA-CAG-mADAMTS13 plasmid.....	37
7.2 <i>In vitro</i> testing of the pMA-CAG-mADAMTS13 plasmid.....	42
7.3 Preparation of the pMA-CAG-mADAMTS13 plasmid .....	43
7.4 Creation of immunodeficient <i>Adamts13</i> knockout mice .....	44
<b>Statistical analysis .....</b>	<b>45</b>
<b>III Results .....</b>	<b>46</b>
<b>8 Diagnosis and prognosis.....</b>	<b>47</b>
8.1 Human ADAMTS13 activity ELISA.....	47
8.2 Human anti-ADAMTS13 autoantibody ELISA .....	49
8.3 Human ADAMTS13 antigen binding ELISA.....	50
<b>9 Gene therapy.....</b>	<b>51</b>

9.1 Construction of the pMA-CAG-mADAMTS13 plasmid.....	51
9.2 <i>In vitro</i> testing of the pMA-CAG-mADAMTS13 plasmid.....	54
9.3 Preparation of the pMA-CAG-mADAMTS13 plasmid .....	54
9.4 Creation of immunodeficient <i>Adamts13</i> knockout mice .....	55
<b>IV Discussion .....</b>	<b>56</b>
<b>10 Diagnosis and prognosis.....</b>	<b>57</b>
10.1 Human ADAMTS13 activity ELISA.....	57
10.2 Human anti-ADAMTS13 autoantibody ELISA .....	57
10.3 Human ADAMTS13 antigen binding ELISA.....	58
<b>11 Gene therapy.....</b>	<b>59</b>
<b>References.....</b>	<b>60</b>
Addendum I Risk Analysis .....	A.1
Addendum II Product information .....	A.2
Addendum III Buffer compositions.....	A.4

Part I

Literature Review

# Chapter 1

## Haemostasis

Human blood is a complex mixture of erythrocytes (red blood cells), leukocytes (white blood cells), thrombocytes (blood platelets) and plasma, which is a watery solution that mainly consists of proteins, carbohydrates, lipids and electrolytes. Erythrocytes take up oxygen from the lungs and transport it via the blood to other tissues. Leukocytes are essential to the body's immune system. Thrombocytes are anucleated cell fragments that are formed in the bone marrow from mature megakaryocytes and are important for haemostasis. Haemostasis is the process that prevents blood loss from damaged vessels by formation of a blood clot (Boron & Boulpaep, 2017; Ruggeri, 2002). At sites of vascular injury, platelets adhere to the subendothelial matrix through interactions with collagen and von Willebrand factor (VWF). First, a primary plug is formed to seal the wound. Eventually, a tightly packed and stable fibrin-rich clot is produced. These two processes are traditionally termed primary and secondary haemostasis, respectively (Versteeg et al., 2013). Haemostasis is typically illustrated by the coagulation cascade model in which proenzymes are converted into active clotting factors by their upstream factor. This cascade consists of two pathways that generate fibrin, the major component of secondary haemostasis (Monroe & Hoffman, 2006; Versteeg et al., 2013). When blood comes into contact with subendothelial cells, the intrinsic pathway of the coagulation system is triggered. The other part of the coagulation system, the extrinsic pathway, starts when tissue factor is released from the lesioned tissue (Boron & Boulpaep, 2017; Versteeg et al., 2013). Clotting, and thus coagulation factors, are contained at the lesion without propagating further along the vessel. Otherwise, this could lead to the occlusion of vessels further down the vascular tree. Moreover, the blood clot is removed after complete wound healing, which is the function of the fibrinolytic system (Monroe & Hoffman, 2006; Versteeg et al., 2013). The fibrinolytic system must maintain balance with the coagulation system to insure normal haemostasis (Chapin & Hajjar, 2015; Ruggeri, 2002). Therefore, haemostasis is tightly regulated by different co-factors, inhibitors, receptors, etc. to prevent pathological thrombus formation or excessive bleeding (Chapin & Hajjar, 2015).

# Chapter 2

## Von Willebrand factor

Von Willebrand factor (VWF) is a large multimeric glycoprotein that is predominantly known for its role in haemostasis. Firstly, VWF causes initial platelet tethering and adhesion to sites of vascular injury, making VWF essential for primary haemostasis. VWF assisted platelet adhesion is especially important when high shear rates are present (Crawley et al., 2011; Reininger, 2008; Stockschlaeder et al., 2014). Secondly, VWF functions as the carrier of coagulation factor VIII (FVIII) thereby stabilizing FVIII and preventing rapid clearance which is crucial for secondary haemostasis (Luo et al., 2012; Sanders et al., 2015; Stockschlaeder et al., 2014). Furthermore, VWF is involved in other processes such as angiogenesis, smooth muscle cell proliferation, tumor cell metastasis and the immune system (Luo et al., 2012). The size and conformation of VWF is essential for its platelet-binding properties, and thus proper functioning (Crawley et al., 2011; Feng et al., 2016; Stockschlaeder et al., 2014). Under normal circumstances the prothrombotic ultra-large (UL) VWF multimers secreted into the circulation are cleaved by ADAMTS13 (A Disintegrin And Metalloproteinase with a Thrombospondin type 1 motif, member 13) into less thrombogenic high molecular weight (HMW) VWF multimers. HMW VWF multimers are the functional VWF multimers needed for haemostasis (Feng et al., 2016; Reininger, 2008; Tersteeg et al., 2015). Mutations that lead to a loss in HMW VWF multimers cause a serious hereditary bleeding disorder known as von Willebrand disease (VWD) type 2A (James & Lillicrap, 2013). Missense substitutions in the VWF gene either interfere with HMW VWF multimer assembly or aid accelerated ADAMTS13 mediated proteolysis (Lillicrap, 2013). VWD type 1 and type 3 are characterized by a quantitative deficiency in VWF multimers (Blombäck et al., 2012). Thus, a qualitative or quantitative defect in VWF causes a serious bleeding implication in VWD patients (Blombäck et al., 2012). In contrast, patients suffering from thrombotic thrombocytopenic purpura (TTP) have a deficiency of ADAMTS13 resulting in the loss of VWF proteolysis. In the microvasculature, this leads to accumulation and unfolding of UL-VWF multimers which causes abnormal aggregation of platelets and subsequent thrombosis (Crawley et al., 2011; Stockschlaeder et al., 2014; Tsai, 2012).

## 1.2 Biosynthesis

VWF is encoded on chromosome 12 and contains 52 exons (Stockschlaeder et al., 2014). As illustrated in Figure 1, the protein is translated as pre-pro-VWF, consisting of a signal peptide (SP), a pro-peptide (D1-D2) and a mature VWF subunit (D'-D3-A1-A2-A3-D4-C1-C2-C3-C4-C5-C6-CK) (Luo et al., 2012; Reininger, 2008).

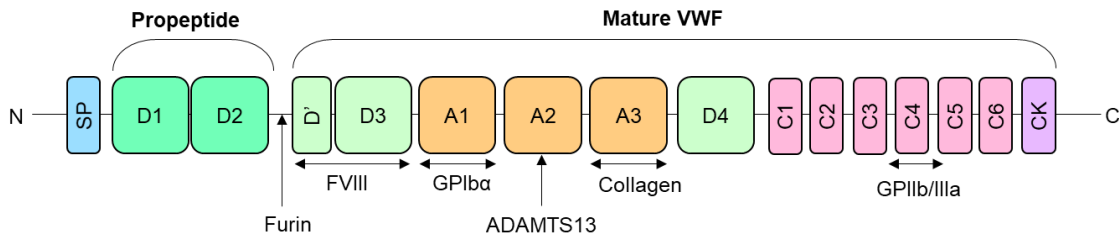


**Figure 1. Domain organisation of VWF.** Pre-pro-VWF consists of a signal peptide (SP), a propeptide (D1-D2) and the mature VWF monomeric subunit (D'-D3-A1-A2-A3-D4-C1-C2-C3-C4-C5-C6-CK). The signal peptide ensures the translocation of pre-pro-VWF to the ER. The propeptide acts as a disulphide isomerase and is removed by furin. The D'-D3 domain non-covalently binds FVIII. The platelet receptor GPIIb interacts with the A1 domain of VWF. The A2 domain contains the ADAMTS13 cleavage site. The A3 domain contains a collagen binding site. The GPIIb/IIIa platelet receptor recognizes the RGD sequence in the C4 domain. The CK domain is important for dimerization of VWF (Figure based on Hovinga Kremer et al., 2017).

However, multimeric VWF is composed out of multiple identical subunits that are linked together with disulphide bonds (Figure 2) (Crawley et al., 2011; Luo et al., 2012; Reininger, 2008). Firstly, pro-VWF is translocated to the endoplasmic reticulum with the help of the signal peptide. After translocation, interpeptide disulphide bonds link cysteines in the C-terminal CK domains to form dimers (tail-to-tail). Subsequently, these dimers are moved to the Golgi apparatus where they undergo further multimerization and glycosylation which is important for secretion of the protein. The multimerization process is catalysed by the pro-peptide, consisting of the D1 and D2 domain, that serves as disulphide isomerase. This N-terminal head-to-head multimerization leads to a spectrum of differentially sized VWF multimers (Crawley et al., 2011; Katsumi et al., 2000; Lenting et al., 2015; Luo et al., 2012).

Synthesis of VWF multimers is exclusive to endothelial cells and megakaryocytes, the precursors of platelets (Luo et al., 2012; Stocksclaeder et al., 2014). Endothelial cells constitutively release VWF multimers that go into the circulation. In addition, these cells store VWF protein in Weibel-Palade bodies. VWF is only secreted after activation of the endothelial cells by secretagogues. VWF is also produced in megakaryocytes and stored in  $\alpha$ -granules until the activation of the platelets (Luo et al., 2012; Reininger, 2008; Stocksclaeder et al., 2014). Before secretion and storage of the mature VWF protein, the pro-peptide is removed by furin (Figure 2) (Crawley et al., 2011; Reininger, 2008).

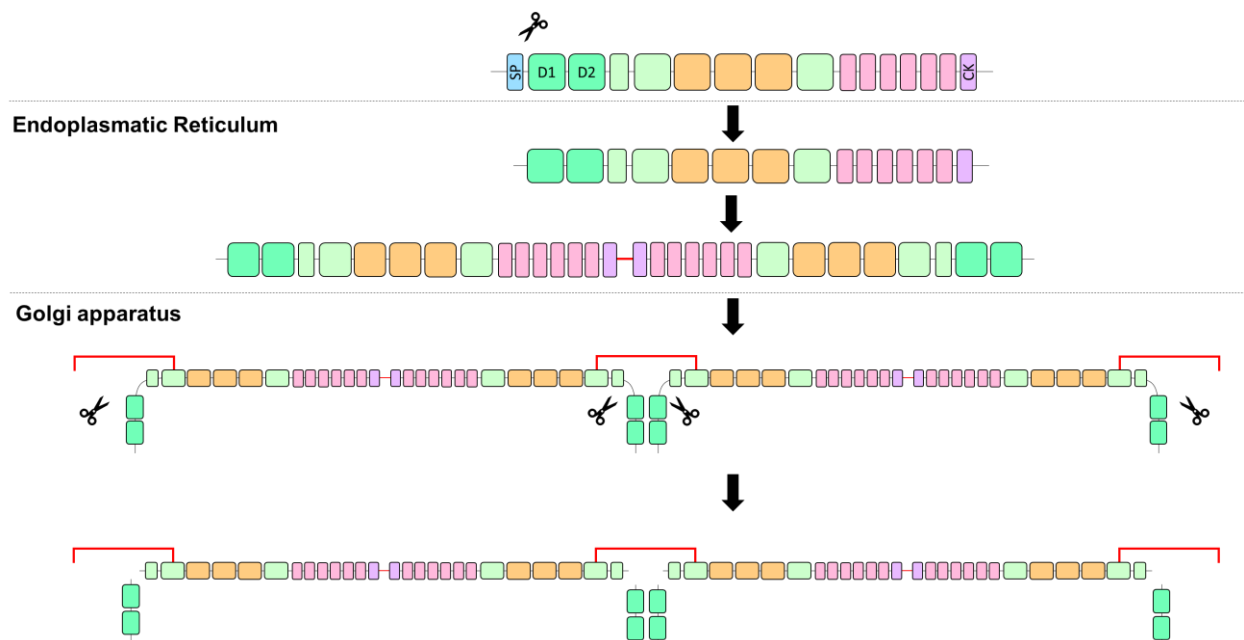


**Figure 2. VWF multimerization.** The VWF gene is translated to pre-pro-VWF and the removal of the signal peptide ensures translocation of pro-VWF to the ER. In the ER, disulphide bridges link the cysteine residues in the CK domains forming dimers in a “tail-to-tail” association. In the golgi apparatus, further multimerization via the N-terminal D3 domains (“head-to-head association”) and extensive glycosylation takes place. Afterwards, the propeptide is removed by furin. (Figure based on Luo et al., 2012; Sadler, 2002).

Stored VWF is rich in UL-VWF multimers that can exceed 20 000 kDa (Katsumi et al., 2000; Lam et al., 2007; Tsai, 2012). However, these extremely prothrombotic multimers are normally not present in circulation (Crawley et al., 2011; Reininger, 2008). Circulating VWF multimers have a molecular weight up to 10 000 kDa and are divided into three groups: high molecular weight (HMW), intermediate molecular weight (IMW) and low molecular weight (LMW) multimers (Figure 3) (Reininger, 2008; Stocksclaeder et al., 2014).

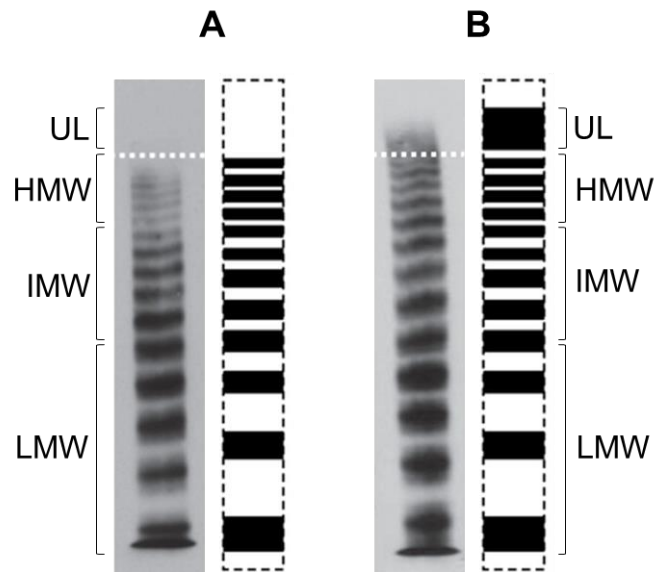


**Figure 3. VWF multimeric pattern of normal human plasma and patient with circulating UL-VWF multimers.**

(A) UL-VWF multimers can only be detected transiently in healthy individuals, shortly after induction of secretion from storage sites, and thus are not detected in the VWF multimeric pattern of normal human plasma. (B) The VWF multimeric pattern of a plasma sample representative for TTP patients confirms the presence of circulating UL-VWF multimers due to the loss of VWF proteolysis (visible above the dashed line). UL = Ultra-large; HMW = High molecular weight; IMW = Intermediate molecular weight; LMW = Low molecular weight. (Figure based on Koyama et al., 2012; Lopes da Silva & Cutler, 2016).

## 2.2 Functional domains

Translated VWF consists of an N-terminal signal peptide composed of 22 amino acids (aa), a pro-peptide of 741 aa and a VWF monomer of 2050 aa. The pro-protein structure is comprised of various functional domains: D1-D2-D'-D3-A1-A2-A3-D4-C1-C2-C3-C4-C5-C6-CK (Figure 1) (Lenting et al., 2015; Luo et al., 2012; Rauch et al., 2013).

### 2.2.1 A domain

VWF contains three A domains, named VWF A1, A2 and A3. The A1 domain contains a binding site for platelet receptor GPIIb/IIIa. This receptor is important for initial adhesion of platelets to the surface, especially when local shear rates are high (Luo et al., 2012; Reininger, 2008; Ruggeri, 2002). The A1 domain also has an alternative collagen binding site (Rauch et al., 2013). The A2 domain contains a cleavage site for the metalloprotease ADAMTS13 at the Tyr1605 - Met1606 (Y1605 - M1606) scissile bond. The A3 domain contains a binding site for subendothelial collagen (Crawley et al., 2011; Luo et al., 2012; Reininger, 2008). VWF has a globular conformation, when normal shear stress is present (Crawley et al., 2011; Lenting et al., 2015; Reininger, 2008). The folded form partially hides the GPIIb/IIIa binding site and

ADAMTS13 cleavage site of the A1 and A2 domain, respectively. In contrast, the collagen binding site in the A3 domain is always exposed (Crawley et al., 2011; Reininger, 2008). This allows VWF to bind subendothelial collagen at sites of vascular injury (Lenting et al., 2015; Reininger, 2008). UL-VWF multimers can unfold at sites of high shear stress when bound to collagen or endothelial cells, or while circulating in the microcirculation. This unravelling makes certain cryptic binding sites in the A1 and A2 domain accessible (Crawley et al., 2011; Reininger, 2008; Stocksclaeder et al., 2014). ADAMTS13 regulates VWF size by cleaving the UL-VWF multimers into smaller and less thrombogenic HMW VWF multimers. HMW VWF multimers are crucial for haemostasis because they have a higher binding affinity for platelets as they unfold more easily and have more binding epitopes than smaller multimers (Crawley et al., 2011; Tsai, 2012; Vanhoorelbeke et al., 2002). Once in circulation, these multimers adopt a folded conformation with hidden A2 domains so they cannot be further proteolyzed (Reininger, 2008; Tersteeg et al., 2015).

## 2.2.2 D domains

As previously indicated, VWF is essential for secondary haemostasis because it serves as a FVIII carrier (Luo et al., 2012; Sanders et al., 2015; Stocksclaeder et al., 2014). VWF non-covalently binds FVIII via the VWF D'-D3 domain to form the so-called VWF/FVIII complex. This interaction stabilizes FVIII, protects it from degradation and guides it to damaged sites (Rauch et al., 2013). The VWF D domains also include the D1 and D2 domains that form the pro-peptide. The pro-peptide acts as a disulphide isomerase in multimerization. This pro-peptide is cleaved from VWF by a furin enzyme before secretion of the mature VWF protein (Crawley et al., 2011; Lenting et al., 2015; Luo et al., 2012). As mentioned above, VWF responds to elevated shears stress by changing its conformation from globular to elongated. Thus, the activation of VWF is force-induced and correlates with its elongation when a certain shear stress is reached. When performing force measurements on VWF dimers, Müller et al. (2016) identified a strong intermonomer interaction involving the D4 domains of the monomers. The complementary domains of the monomers are thought to align side-by-side and become closely associated due to the D4-D4 interaction. This compact arrangement shortens the actual length of VWF. Subsequently, the strong D4-D4 interaction may tune VWF's sensitivity to the hydrodynamic flow as it will only dissociate and allow VWF to elongate at high forces. The general structure of a D domain includes a von Willebrand domain, a cysteine-8 structure and a trypsin-inhibitor-like-fold (Rauch et al., 2013; Zhou et al., 2012).

## 2.2.3 C domains

The C-terminal part of the protein contains six C domains, named C1, C2, C3, C4, C5 and C6 (Zhou et al., 2012). Initially, VWF tethers platelets to the surface through interaction with GPIIb $\alpha$ . Then, platelet activation occurs and causes a conformational change in platelet integrin

$\alpha$ IIb $\beta$ 3, also called GPIIb/IIIa. This platelet receptor recruits soluble proteins, such as VWF and fibrinogen, which then bind other platelets. The integrin causes stable platelet-platelet and platelet-vessel adhesion (Luo et al., 2012; Rauch et al., 2013; Ruggeri, 2002).  $\alpha$ IIb $\beta$ 3 recognizes the Arginine-Glycine-Aspartic acid (RGD) motif in the C4 domain of VWF. Hence, C4 is important for the formation of a stable clot (Rauch et al., 2013). VWF is the only ligand that is able to bind both GPIb $\alpha$  and GPIIb/IIIa (Luo et al., 2012).

## 2.2.4 CK domain

Cysteines account for 8.3% of the VWF amino acid content. Accordingly, intrapeptide as well as interpeptide disulphide bonds are of great importance. The CK or CTCK domain contains 11 cysteines and as mentioned above, is essential for tail-to-tail VWF dimerization. The domain is positioned C-terminally and is similar to certain members of the cystine knot (CK) family. Hence, the name C-terminal cystine knot-like or CTCK domain (Katsumi et al., 2000). A cystine knot typically contains two disulphide bonds that “perpendicularly” link two  $\beta$  strands through which a third disulphide is threaded (Zhou et al., 2012).

# Chapter 3

## ADAMTS13

In 1996, ADAMTS13 (A Disintegrin And Metalloproteinase with a Thrombospondin type 1 motif, member 13) was partially purified from normal human plasma for the first time. Furlan et al. (1996) and Tsai (1996) described ADAMTS13 as a “metalloproteinase” or “metalloenzyme” that could cleave VWF. Therefore, the protein became known as VWFCP or von Willebrand factor cleaving protease (Zheng, 2015). In 2001, Zheng et al. and Levy et al. identified VWFCP as the 13th member of the ADAMTS family of zinc dependent metalloproteases, hence its new name: ADAMTS13. VWF is the only known substrate of ADAMTS13 and proteolysis of VWF is crucial for regulation of thrombogenesis (Feng et al., 2016; Levy et al., 2001; Zheng et al., 2001). The multiple interactions between ADAMTS13 and VWF ensure a highly specific recognition (Crawley et al., 2011). ADAMTS13 deficiency, apparent in patients with thrombocytopenic thrombotic purpura (TTP), causes accumulation of UL-VWF multimers which can lead to platelet aggregation and formation of thrombi in the microcirculation (Feng et al., 2016; Zander et al., 2015). ADAMTS13 may also be involved in the regulation of inflammation and angiogenesis, as well as the degradation of the extracellular matrix (Feng et al., 2016).

### 3.1 Functional domains

ADAMTS13 is encoded on the long arm of chromosome 9q34 and contains 29 exons (Levy et al., 2001; Zheng, 2015). The protein is mainly synthesized by hepatic stellate cells. However, ADAMTS13 is also found in smaller amounts in other cells, including vascular endothelial cells, megakaryocytes, platelets, renal tubular epithelial cells, glomerular endothelial cells and glomerular podocytes (Crawley et al., 2011; Feng et al., 2016; Zheng, 2013). All members of the ADAMTS family contain a signal peptide (SP) and a propeptide (P), as well as a metalloprotease domain (M), a disintegrin-like domain (D), a thrombospondin type-1 repeat (T1), a cysteine-rich domain (C) and a spacer domain (S). In addition, ADAMTS13 contains seven other thrombospondin type-1 repeats (T2-T8) and two CUB (complement components C1r/C1s, Uegf and Bmp1) domains (Figure 4) (Crawley et al., 2011; Ercig et al., 2018; Kremer Hovinga et al., 2017). The nascent ADAMTS13 precursor protein is composed of 1427 aa (Lämmle et al., 2005). While traveling through the ER and the Golgi apparatus, the signal peptide and propeptide are removed and the mature ADAMTS13, consisting of 14 domains, is formed (Roose et al., 2018a; Zheng, 2015). The mature protein has a molecular weight of approximately 190 kDa and has an estimated concentration of 1 µg/mL in normal plasma (Ercig et al., 2018; Feys et al., 2006; Muia et al., 2014; Roose et al., 2018a). Although it was

believed that ADAMTS13 enters the blood as a constitutively active enzyme, because of the lack of a cysteine switch (see below 3.1.1) (Plautz et al., 2018), it is now known that the protein is present in a folded, low-activity conformation due to an interaction between its spacer and CUB domains and that it adopts an open conformation after binding to the D4-CK domains of VWF (Ercig et al., 2018; Muia et al., 2014; South et al., 2014).

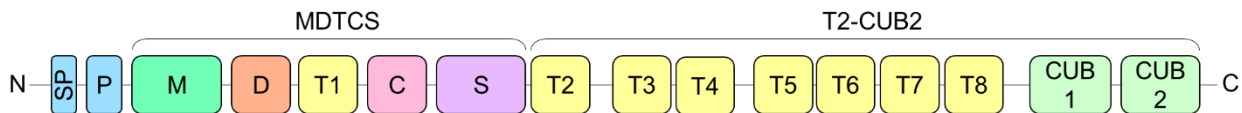


**Figure 4. Domain organisation of ADAMTS13.** ADAMTS13 consists of a signal peptide (SP), a propeptide (P), a metalloprotease domain (M), a disintegrin-like domain (D), 8 thrombospondin type-1 repeats (T1-T8), a cysteine-rich domain (C), a spacer (S) domain and 2 CUB domains (CUB1 and CUB2). The N-terminal part of ADAMTS13 is called MDTCS and the C-terminal part T2-CUB2. (Figure based on Hovinga Kremer et al., 2017).

### 3.1.1 Propeptide

ADAMTS13 contains a propeptide of 41 aa, which is unusually short in comparison to the propeptide of other ADAMTS family members. Surprisingly, this short propeptide is not required for secretion or activation of ADAMTS13 (Zheng, 2013). The propeptide of the other ADAMTS proteases functions as a “cysteine switch” which blocks the active site of the protease until conversion to its active form. Consequently, absence of this switch in the propeptide of ADAMTS13 causes the protein to be secreted as a “constitutively active” enzyme (Ercig et al., 2018; Plautz et al., 2018; Zheng, 2013).

### 3.1.2 Metalloprotease domain

The metalloprotease domain contains the active site. As mentioned above, the cysteine-zinc ion interaction apparent in the cysteine switch of most ADAMTS family members is not involved in the regulation of the catalytic activity of ADAMTS13 (Ercig et al., 2018). However, the coordination of a zinc ion in the catalytic cleft is still essential for the catalytic function of ADAMTS13. Accordingly, ADAMTS13 contains the HEXXHXXGXXHD sequence expected in a reprolysin(-like) metalloprotease. This motif contains three histidine residues that coordinate the zinc ion in the active site (Ercig et al., 2018; Zheng, 2013). The zinc ion facilitates cleavage of VWF by interaction with a glutamine residue (Glu225) in the active site. A methionine residue (Met249) forms a “Met-turn” that creates a hydrophobic environment for the histidine residues (Ercig et al., 2018). The metalloprotease domain also contains three putative calcium binding sites. The first and second site form a calcium cluster and the residues in the first site seem to

provide low-affinity  $\text{Ca}^{2+}$  binding. The third site, however, provides high-affinity  $\text{Ca}^{2+}$  binding and seems to be important for the proteolytic activity of ADAMTS13. This might result from the location of the third site, which is close to the active site (Ercig et al., 2018; Zheng, 2013). Studies performed by Anderson et al. (2006) showed that ADAMTS13 activity is enhanced 2-fold by addition of zinc ions, 3-fold by addition of calcium ions and 6-fold when both ions are added to citrated plasma. This suggests that the two divalent cations may indeed play a cooperative role in supporting ADAMTS13 activity (Anderson et al., 2006). The metalloprotease domain also contains three variable regions (Glu184-Arg193; Phe216-Val220; Gly236-Ala261) that are important for substrate specificity. Three specific subsites, named the S1 pocket (Leu151/Val195), the S1' pocket (Asp252-Pro256) and S3 subsite (Leu198, Leu232 and Leu274) recognize VWF (Crawley et al., 2011).

Of note, the studies performed by Anderson et al. (2006) also suggest that the use of citrate as an anticoagulant in blood products is not optimal when ADAMTS13 activity levels need to be measured as citrate inhibits ADAMTS13 activity by chelating  $\text{Ca}^{2+}$  and  $\text{Zn}^{2+}$ . However, they suggest that heparin, a nonchelating anticoagulant, would be an acceptable alternative as the addition of heparin to plasma results in normal ADAMTS13 activity (Anderson et al., 2006). Heparin catalyses the endogenous inhibiting effect of antithrombin, and thus works indirectly on the clotting cascade. Antithrombin binds and inhibits several enzymes of the coagulation cascade, including thrombin (factor IIa) and factor Xa, a process that normally occurs at slow rate. However, heparin accelerates this effect a 4000- and 1200-fold respectively (Finley & Greenberg, 2013).

### 3.1.3 Disintegrin-like domain

Disintegrins are small polypeptides found in snake venom. The disintegrin-like domain of ADAMTS13 shares similarities with disintegrins, but does not function like a disintegrin domain due to the absence of the typical RGD sequence that can bind with high affinity to integrin receptors (Crawley et al., 2011; Ercig et al., 2018). The disintegrin-like domain is positioned close to the catalytic cleft and forms a functional unit with the metalloprotease domain (Crawley et al., 2011; Zheng, 2013). The disintegrin-like domain is important for substrate recognition, together with the cysteine-rich and spacer domain. Exosite-1, spanning residue 332 to residue 364, contain the Arg349 and Leu350 residues that may interact with the Asp1614 and Ala1612 residues in the A2 domain of VWF, respectively (Ercig et al., 2018; Zheng, 2013). This would aid the correct positioning of the Y1605 - M1606 scissile bond for cleavage (Zheng, 2013).

### 3.1.4 Cysteine-rich domain

As mentioned above, both the cysteine-rich and spacer domain are essential for the recognition of VWF. The cysteine-rich domain of ADAMTS13 contains 10 conserved cysteines, hence the name (Crawley et al., 2011). The domain shares homology with the cysteine-rich domain of other ADAMTS family members, but the sequence that is not conserved seems to be most crucial for its function. This region contains exosite-2 (Gly471-Ala472-Ala473-Val474) which forms a hydrophobic pocket that is important for interactions with the VWF A2 domain, including the predicted interaction of Pro475 with the VWF Trp1644 residue (de Groot et al., 2015; Ercig et al., 2018). Furthermore, the hydrophobic pocket is suggested to be important for proteolysis (de Groot et al., 2015).

### 3.1.5 Spacer domain

The spacer domain is 130 aa long and contains exosite-3. Exosite-3 contains Tyr658, Arg659, Arg660, Tyr661, Tyr665, as well as Arg568 and Phe592 (Ercig et al., 2018; Zheng, 2013). These residues form a hydrophobic cluster at the surface of ADAMTS13, and thus easily interact with residues Glu1660-Arg1668 of the VWF A2 domain when it becomes unfolded by shear stress (Crawley et al., 2011; Ercig et al., 2018). The spacer domain exists of 10  $\beta$ -strands in a jelly roll topology that form 2 antiparallel  $\beta$ -sheets (Crawley et al., 2011). Recently, the interaction between the spacer and CUB domains was demonstrated to play a leading role in the autoinhibition of ADAMTS13, which is disrupted by binding to VWF (Muia et al., 2014; South et al., 2014).

### 3.1.6 Thrombospondin Type-1 Repeats

ADAMTS13 contains eight thrombospondin type-1 repeats (T1 to T8) that share great homology with the repeat found in thrombospondin-1 and thrombospondin-2. The first repeat is located between the disintegrin-like domain and the cysteine-rich domain and the seven other repeats are located downstream of the spacer domain (Crawley et al., 2011). The repeats are involved in cellular localization and recognition of VWF, e.g. T1 binds to VWF73, which spans residues Asp1596 to Arg1668 of VWF (Zheng, 2013).

### 3.1.7 CUB domains

CUB domains are found in proteins that are important for developmental regulation, such as bone morphogenic protein 1 (Bmp1) (Crawley et al., 2011). The acronym was deviated from three proteins, namely the complement components C1r/C1s, Uegf (urinary epidermal growth factor-related sea urchin protein) and Bmp1 (bone morphogenic protein 1). The two CUB domains found in ADAMTS13 are homologous and have a highly conserved sequence, except

for the C-terminal region of the CUB2 domain (Deforche et al., 2016; Ercig et al., 2018). T5-CUB2 may bind to the D4-CK region of VWF (Crawley et al., 2011).

## 3.2 Interaction of ADAMTS13 and VWF

At low shear stress, ADAMTS13 and VWF can circulate as a complex via weak interactions between the C-terminal T5-CUB2 region of ADAMTS13 and the C-terminal D4-CK domains of VWF (Figure 5A) (Crawley et al., 2011; Plautz et al., 2018). The VWF D4-CK plays a critical role in correctly positioning ADAMTS13 at the VWF A2 domain and changes the conformation of ADAMTS13 from a “closed” to “open” conformation that enables it to cleave VWF (South 2017). As mentioned above, shear stress changes the conformation of (UL-)VWF multimers resulting in the exposure of the Y1605 - M1606 cleavage site in the A2 domain. Recently, it was shown that ADAMTS13 also undergoes a conformational change from a globular folded state to an open active state (South et al., 2017). This change is needed for ADAMTS13 to gain the ability to cleave VWF at the Y1605 - M1606 scissile bond (South et al., 2014). VWF allosterically regulates this change in conformation (Muia et al., 2014). Thus, rather than circulating as a constitutively active protein, as hypothesized previously, ADAMTS13 enters the blood in a closed and low-activity state (Ercig et al., 2018). The closed conformation is mediated through interaction of the CUB domains with the spacer domain (Muia et al., 2014; South et al., 2017). The spacer domain, that contains exosite-3, is essential for VWF recognition as it interacts with the VWF A2 domain. Exosite-3 is only available for interaction with and recognition of the VWF A2 domain in the open formation of ADAMTS13 (Ercig et al., 2018). Therefore, the interaction of the CUB domains with the spacer domain causes autoinhibition. Upon interaction of the D4-CK domains of VWF with the C-terminal domains of ADAMTS13, this inhibition is relieved and ADAMTS13 becomes fully activated. The D4-CK domain also plays a role in correctly positioning ADAMTS13 at the A2 domain (Crawley et al., 2011; South et al., 2017). Once this interaction is established (Figure 5 A), other complementary exosites on VWF and ADAMTS13 are allowed to interact in a step-by-step manner (South et al., 2017). This series of steps eventually leads to the proteolysis of VWF and is called the “molecular zipper mechanism” (Figure 5). Under elevated shear flow, VWF can unfold which enables the spacer domain to bind the A2 domain (Figure 5 B and C) (Crawley et al., 2011; South et al., 2017). This interaction brings the two molecules closer to each other, which allows exosite-1 of the disintegrin-like domain to interact with VWF (Figure 5 D) (de Groot et al., 2015). The exosite-1-VWF interaction assist the Y1605 - M1606 bond into the catalytic cleft (de Groot et al., 2010). Accordingly, the subsites of the metalloprotease domain can interact with their complementary residues on VWF. The S3 subsite interacts with the Leu1603 residue of VWF. Thereafter, the Y1605 and the M1606 residues of the scissile bond interact with the S1 and S1' subsite pocket, respectively (Figure 5 E). Finally, the Y1605

- M1606 bond in the VWF A2 domain is cleaved by ADAMTS13 (Figure 5 F) (Crawley et al., 2011).

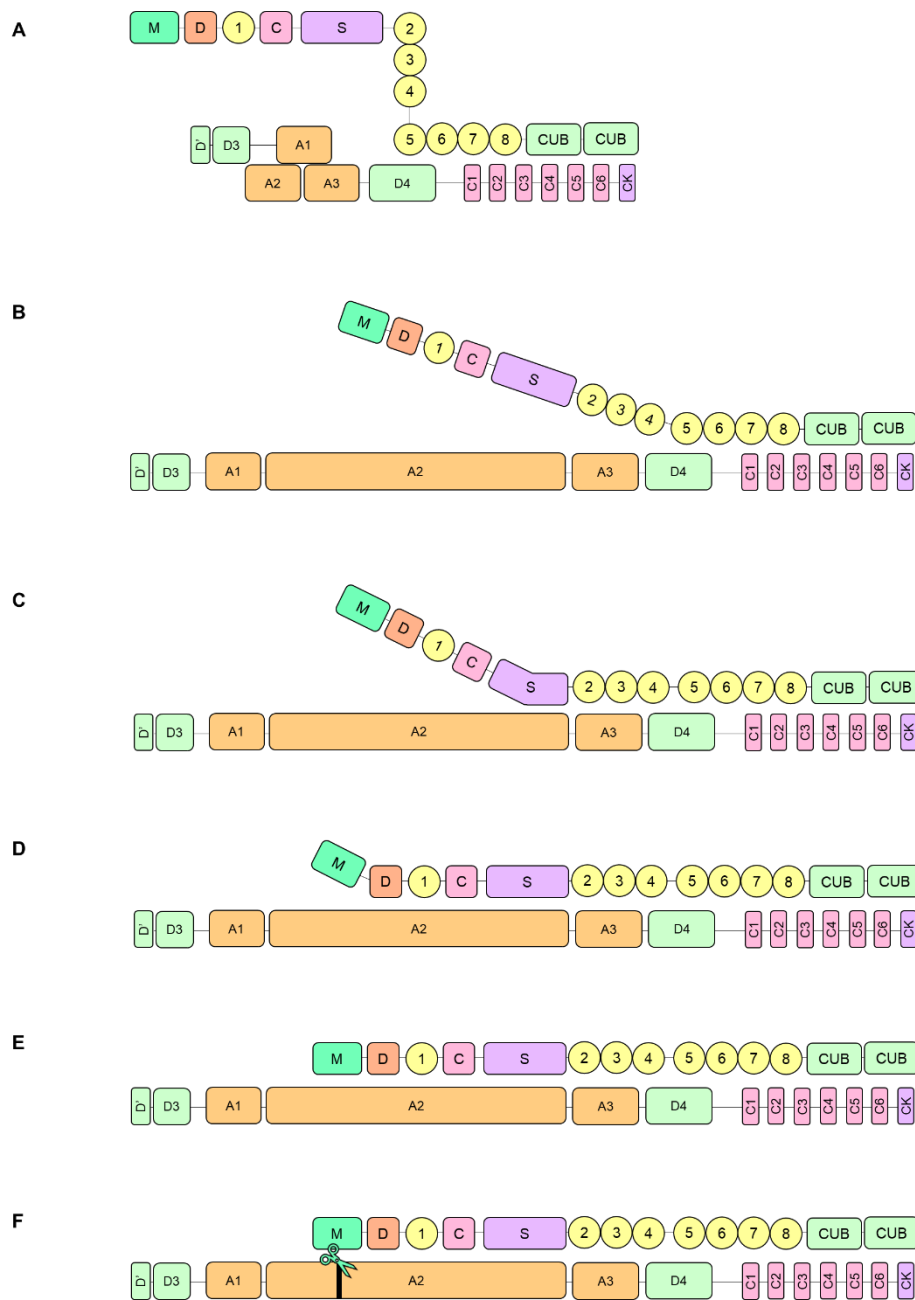


**Figure 5. The proteolysis of VWF by ADAMTS13 via the molecular zipper mechanism.** (A) Globular VWF is bound by ADAMTS13 in circulation via the VWF D4-CK domains and the ADAMTS13 T2-CUB2 region. (B) When high shear rates are present, the A2 domain of VWF unfolds. (C) Residues of exosite-3 in the ADAMTS13 S domain interact with the C-terminal part of the VWF A2 domain. (D) Residues of exosite-1 of the ADAMTS13 D domain interact with VWF. This aids the Y1605 - M1606 (VWF A2 domain) into the catalytic cleft. (E) The S3 subsite of the M domain interacts with the L1603 residue of VWF and the S1 and S1' subsites interact with the Y1605 and M1606 residue, respectively. (F) Finally, the proteolysis of the Y1605 - M1606 bond in the VWF A2 domain occurs. (Crawley et al., 2011).

# Chapter 4

## Thrombotic thrombocytopenic purpura

Thrombotic thrombocytopenic purpura (TTP) is a rare thrombotic microangiopathy (TMA) with a prevalence of approximately ten per million people per year and a mortality rate exceeding 90% when left untreated (Joly et al., 2017a; Sadler, 2002). The first case of TTP was described by Dr. Eli Moschcowitz and was assigned to an agglutinative and haemolytic poison. His patient was presented with an acute onset of fever, petechiae (red-purple dots), anaemia, paralysis, coma, and died within two weeks. At the autopsy, small clots were found in the patient's microvasculature (Plautz et al., 2018; Zander et al., 2015). In 1982, Moake et al. hypothesized that the formation of these microthrombi was caused by the presence of UL-VWF multimers in the plasma of TTP patients. It was postulated that these multimers accumulated due to a deficiency in a VWF "depolymerase" (Moake et al., 1982; Zheng, 2015). In 1996, this "depolymerase" was discovered simultaneously by Furlan and Tsai, namely ADAMTS13 (Furlan et al., 1996; Tsai, 1996; Zheng, 2015). It is now accepted that a severe deficiency in ADAMTS13 (ADAMTS13 activity <10%), either constitutional or acquired, is specific to TTP (Joly et al., 2017a; Zheng, 2015). However, certain environmental and/or genetic triggers are needed for the onset of an acute TTP episode. Thus, not all patients with severe ADAMTS13 deficiency spontaneously develop the disease (Vanhoorelbeke & De Meyer, 2013). Nevertheless, patients that survive a first acute episode are at high risk for relapse, stressing the need to consider TTP as a chronic disease (Coppo et al., 2019).

### 4.1 Pathophysiology

Under normal circumstances, UL-VWF multimers spontaneously unfold in circulation due to high local shear forces, e.g. in the microvasculature, and are cleaved by ADAMTS13 into less thrombogenic VWF multimers (Crawley et al., 2011; Vanhoorelbeke & De Meyer, 2013). When patients have a deficiency in ADAMTS13, UL-VWF multimers accumulate and form platelet aggregates, leading to the formation of VWF- and platelet-rich microthrombi (Joly et al., 2017; Sadler, 2017). As a result of partial occlusion of small blood vessels, organ ischemia may occur, especially in the brain, heart, gastrointestinal tract and kidneys (Blombery & Scully, 2014; Kremer Hovinga et al., 2017b). The development of multiple organ failure rapidly becomes fatal and patients die within days or weeks after disease onset. Furthermore, the microthrombi cause haemolytic anaemia with fragmented red blood cells (schistocytes), as well as thrombocytopenia due to deprivation of thrombocytes in the blood (Kremer Hovinga et al., 2017).

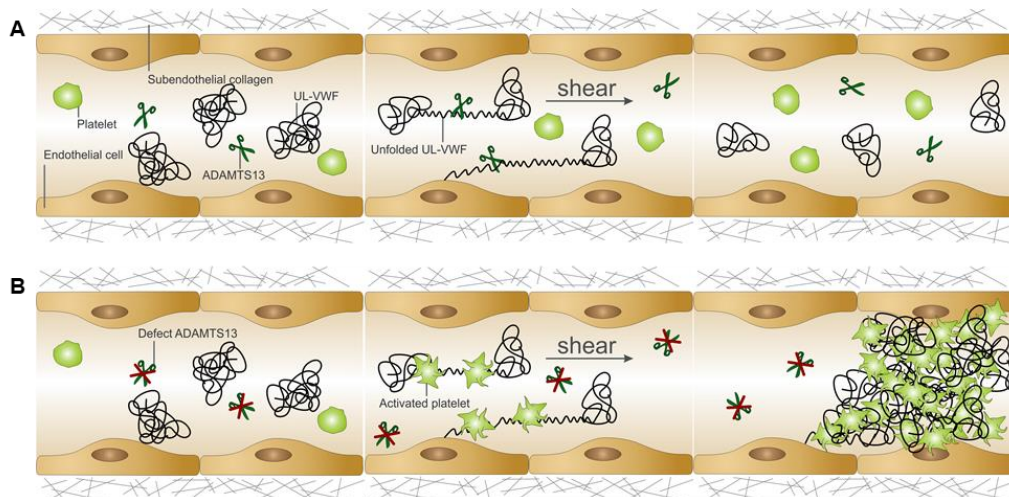


**Figure 6. Pathophysiology of TTP.** (A) In a healthy individual, UL-VWF multimers unfold in the blood flow due to shear stress and are cleaved by ADAMTS13 (green scissors) into less thrombogenic HMW VWF multimers. (B) TTP patients have a severe deficiency of ADAMTS13 due to anti-ADAMTS13 antibodies (not shown) or mutations in the *ADAMTS13* gene causing less secretion of the enzyme (not shown) or a dysfunctional form (“Defect ADAMTS13”). Consequently, the UL-VWF multimers are not cleaved, they accumulate and bind platelets. Eventually, this leads to the formation of microthrombi in the small blood vessels that can occlude these vessels. (Figure made by L. Deforche).

## 4.2 Congenital and immune-mediated TTP

In a minority of TTP patients (5%), severe deficiency of ADAMTS13 is the result of mutations in the *ADAMTS13* gene (congenital TTP; cTTP). In approximately 95% of the cases, severe deficiency of the enzyme is caused by anti-ADAMTS13 autoantibodies (immune-mediated TTP; iTTP). These autoantibodies affect the proteolytic activity and/or clearance of ADAMTS13 (Kremer Hovinga et al., 2017). In 50% of all patients, no associated aetiology is observed and the patients are diagnosed with “primary” or “idiopathic” TTP. The remaining 50% of the patients have a pre-existing or concomitant condition, and are diagnosed with “secondary” or “non-idiopathic” TTP. These concomitant conditions, including pregnancy, autoimmune diseases, bacterial infections, human immunodeficiency virus (HIV) infection, pancreatitis, cancer, organ transplantation and drug use, are often associated with high shear rates and therefore potentially trigger the acute TTP episodes (Blombery & Scully, 2014; Joly et al., 2017a; Knöbl, 2018). The manifestation of the first acute TTP episode varies extremely between cases, with 90% onset in adulthood and 10% onset during childhood or adolescence. Childhood-onset is relatively more frequent in patients suffering from cTTP (Joly et al., 2017a).

## 4.2.1 Congenital TTP

Congenital TTP, or Upshaw–Schulman syndrome, is linked to homozygous or compound heterozygous mutations in the ADAMTS13 gene located on chromosome 9q34 (Kremer Hovinga et al., 2017; Lämmle et al., 2005). More than 150 different mutations have been identified including missense, nonsense, splice site, and frameshift mutations (Kremer Hovinga et al., 2017; Plautz et al., 2018). The majority of these mutations (86%) affect the secretion of ADAMTS13. However, mutations causing a decrease in the proteolytic activity of the enzyme have also been detected (Lotta et al., 2010; Underwood et al., 2016). The mutations span the entire ADAMTS13 gene, but are mainly found within the N-terminal region (Joly et al., 2017a). In addition, gene polymorphisms of ADAMTS13 might also be responsible for differences in ADAMTS13 deficiency, particularly in combination with mutations (Lotta et al., 2010). The genetic heterogeneity of cTTP is reflected in the variable disease course of these patients, including differences in frequency and severity of the TTP episodes, as well as the bimodal distribution of disease onset: cTTP can appear early in childhood, by the age of 2-5, or remain asymptomatic until later in adulthood, often until 20-40 years of age (Blombery & Scully, 2014; Kremer Hovinga & Lämmle, 2012; Kremer Hovinga et al., 2017). In women, the initial acute episode frequently appears during the third trimester of the first pregnancy, when an increase in fibrinogen and VWF levels is detected, as well as a decrease in ADAMTS13 activity (Plautz et al., 2018). Other pathophysiological conditions that increase VWF levels, e.g. inflammation and sepsis, can also trigger an acute TTP episode (Joly et al., 2017a). Moreover, cTTP patients have a high risk of chronic relapsing after their first acute TTP episode and therefore long-term follow-up is recommended (Kremer Hovinga & Lämmle, 2012; Joly et al., 2017a).

## 4.2.2 Immune-mediated TTP

Immune-mediated TTP is an autoimmune disorder caused by anti-ADAMTS13 autoantibodies. Anti-ADAMTS13 autoantibodies are predominantly of the immunoglobulin G (IgG) class, particularly the IgG4 and IgG1 subclasses, although autoantibodies of the IgM and IgA class have also been reported (Ferrari et al., 2014; Kremer Hovinga et al., 2017). Furthermore, two different types of anti-ADAMTS13 autoantibodies have been detected in iTTP patients, namely inhibitory autoantibodies that inhibit the proteolytic activity of ADAMTS13 and non-inhibitory autoantibodies that accelerate clearance of ADAMTS13 (Thomas et al., 2015). Although the immune response against ADAMTS13 is polyclonal, autoantibodies against the spacer domain are found in almost all iTTP patients (Kremer Hovinga & Lämmle, 2012; Thomas et al., 2015). Moreover, the spacer domain is the primary target for inhibitory autoantibodies (Thomas et al., 2015). Nevertheless, clearance of ADAMTS13, rather than inhibition of enzyme function, appears to be the main mechanism causing the decrease in ADAMTS13 activity (Feys et al., 2006; Thomas et al., 2015). Moreover, binding of antibodies to ADAMTS13 leads to the formation of circulating antigen-antibody complexes or immune complexes (CICs) that can

persist for years, even after remission. These CICs are enzymatically inactive and assist the accelerated clearance of ADAMTS13 (Ferrari et al., 2014; Kremer Hovinga et al., 2017; Thomas et al., 2015). CICs are also detected in other autoimmune diseases where they promote inflammation and tissue damage (Ferrari et al., 2014; Mancini et al., 2017). Additionally, it is known that the conformational change and the subsequent exposure of cryptic epitopes in a protein can lead to the formation of autoantibodies against that protein, which is the case in certain autoimmune diseases, e.g. antiphospholipid syndrome (de Laat et al., 2011) and heparin induced thrombocytopenia (Kreimann et al., 2014). In 2014, South et al. and Muia et al. showed that ADAMTS13 adopts an open conformation when allosterically activated by VWF. South et al. also suggested that the open conformation results in the exposure of cryptic epitopes in the spacer domain, which are shielded by the CUB domains in the closed conformation. Recently, Roose et al. (2018a) showed that ADAMTS13, that normally circulates in a folded conformation, is open in iTTP patients when suffering from an acute TTP episode. Roose et al. (2018b) also showed that iTTP patients indeed possess anti-ADAMTS13 autoantibodies directed against the exposed cryptic epitopes in ADAMTS13. This indicates the significance of in-depth research concerning the question of whether autoantibodies targeting the cryptic epitopes in the spacer domain cause ADAMTS13 deficiency or whether other autoantibodies targeting other domains and/or recognizing non-cryptic epitopes might also be pathogenic. This question is especially important as 5% of the healthy population also have antibodies directed against ADAMTS13 (Grillberger et al., 2014). Finally, certain genetic factors have been associated with a higher risk of developing iTTP, namely female sex, black ethnicity, a human leukocyte antigen (HLA) class II allele (HLA-DRB1\*11) and obesity (Joly et al., 2017a). As with cTTP, certain conditions such as pregnancy, sepsis and inflammation, as well as concomitant autoimmune manifestations and disorders, could potentially trigger an episode in iTTP patients (Joly et al., 2017a; Kremer Hovinga et al., 2017).

## 4.3 Diagnosis

### 4.3.1 Clinical presentation

In 1966, Amorosi and Ultmann established a pentad of diagnostic criteria for TTP patients, including fever, thrombocytopenia associated with haemorrhage and purpura (Figure 7 A), microangiopathic haemolytic anaemia with schistocytes on the blood smear (Figure 7 B), neurological symptoms and renal dysfunction (Amorosi & Ultmann, 1966; Kremer Hovinga et al., 2017). However, recent studies showed that less than 10% of the patients demonstrate all five symptoms when having an acute TTP episode. Nonetheless, almost all patients present with thrombocytopenia and microangiopathic anaemia with schistocytes on the blood smear (Joly et al., 2017a). Signs associated with the red blood cell fragmentation are free serum haemoglobin and elevated lactate dehydrogenase (LDH) levels (Knöbl, 2018). Early symptoms of TTP are often flu-like, such as fatigue, abdominal pain and muscle pain (Coppo et al., 2019). Furthermore, TTP patients are presented with clinical manifestations related to systemic microvascular ischemia. Sixty percent of the patients display neurological symptoms including confusion, headaches, seizures and coma (Blombery & Scully, 2014; Joly et al., 2017a). Symptoms related to heart and mesenteric ischemia include arrhythmias, myocardial infarction, increased serum troponin levels, as well as abdominal pain, diarrhoea and vomiting. Although acute renal failure is rare, it is not insignificant as 10% to 27% acute kidney injury is seen in patients with severe TTP (Joly et al., 2017a; Kremer Hovinga et al., 2017).

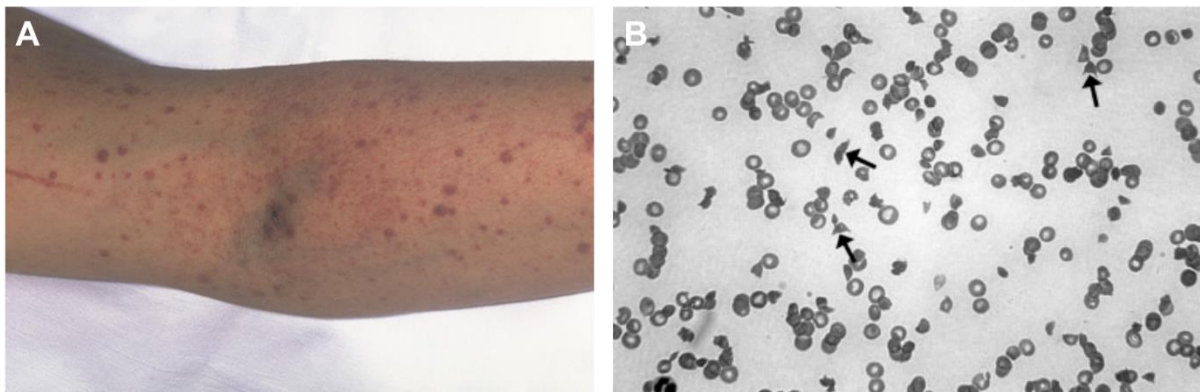


**Figure 7. Clinical signs and symptoms of TTP.** (A) In certain cases, consumption thrombocytopenia allows damaged vessels to leak blood, causing gastrointestinal haemorrhage (not shown) and small red-purple dots on the skin, called purpura (bruises) and petechiae (red and purple dots) (Blombery & Scully, 2014). Digital image retrieved from National Heart, Lung, and Blood Institute; National Institutes of Health; U.S. Department of Health and Human Services. <https://www.nhlbi.nih.gov/health-topics/thrombotic-thrombocytopenic-purpura>. (B) Blood smear of TTP patient with fragmented red blood cells (schistocytes) (arrows). (Figure taken from Lämmle et al., 2005).

### 4.3.2 Differential diagnosis

The rarity of the disease, the variability in clinical presentation of TTP and the overlap with other disorders, especially other TMAs, make TTP diagnosis extremely difficult (Grall et al., 2017; Kremer Hovinga et al., 2017). TMAs that result in similar manifestations include haemolytic uraemic syndrome (HUS), drug-associated TMA and TMA associated with haematopoietic stem cell transplantation, disseminated neoplasia, HIV infection or connective tissue disorders, as well as pregnancy-induced TMA, including pre-eclampsia and HELLP (haemolysis, elevated liver enzymes and low platelets) syndrome (Kremer Hovinga et al., 2017). The diagnosis of TMA is made when a patient presents with microangiopathic haemolytic anaemia and thrombocytopenia. Provided that no alternative aetiology is apparent, or can be concluded from thorough examination of the patient's history, TTP diagnosis can be suspected (Coppo et al., 2019; Joly et al., 2017a; Knöbl, 2018). However, a differential diagnosis can only be made when ADAMTS13 activity is below 10% as severe deficiency in ADAMTS13 is the only specific biomarker for TTP, and thus the only diagnostic feature that can differentiate it from other TMAs (Figure 8) (Joly et al., 2017a). The patient is diagnosed with acquired TTP when ADAMTS13 activity is <10% during the acute TTP episode, but becomes detectable in remission. Thus, as illustrated in Figure 8, a patient with ADAMTS13 activity <10% during an episode and detectable anti-ADAMTS13 autoantibodies is diagnosed with iTTP. When ADAMTS13 activity is <10% but no anti-ADAMTS13 autoantibodies are detected, even during remission, the patient is diagnosed with acquired TTP of an unknown mechanism. The patient is diagnosed with cTTP when ADAMTS13 activity is always <10%, no anti-ADAMTS13 autoantibodies are detected and the *ADAMTS13* gene possesses homozygous or compound heterozygous mutations. In exceptional cases, ADAMTS13 activity is always <10% and no autoantibodies are detected but no mutations in the *ADAMTS13* gene are observed, the patient is then diagnosed with TTP of unknown aetiology (Joly et al., 2017a; Knöbl, 2018).

The ADAMTS13 assays are often performed in a specialized reference laboratory. Therefore, the results are generally not directly available to the hospital (Sadler, 2015). The complexity of the diagnostic process and the time it takes to perform and analyse the crucial activity assays, can lead to delays in TTP diagnosis and misdiagnosis of TTP patients (Coppo et al., 2019; Grall et al., 2017).

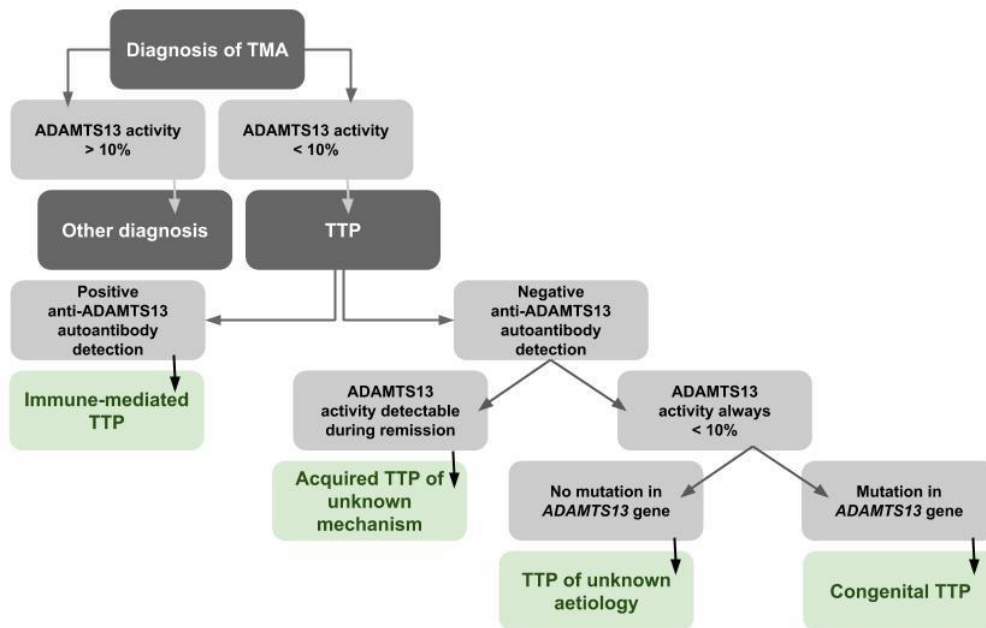


**Figure 8. Flowchart for diagnosis of TTP.** Firstly, ADAMTS13 activity is the only unique biomarker to differentiate TTP from other TMAs and diagnosis of TTP is confirmed when ADAMTS13 activity is <10%. Next, the anti-ADAMTS13 autoantibody (anti-ADAMTS13 IgG) screening is performed. Presence of anti-ADAMTS13 autoantibodies during the acute episode or remission confirms iTTP. When ADAMTS13 activity spontaneously recovers during remission but no anti-ADAMTS13 IgG are detected, the patient is diagnosed with acquired TTP of an unknown mechanism. The patient is diagnosed with cTTP when ADAMTS13 activity is always <10%, detection of anti-ADAMTS13 IgG's is always negative and the *ADAMTS13* gene possesses mutations. When ADAMTS13 activity is always <10%, no anti-ADAMTS13 IgG's are detected and *ADAMTS13* gene analysis shows no mutations in the gene, the patient is then diagnosed with TTP of unknown aetiology. (Figure based on Joly et al., 2017a).

### 4.3.3 Prognostic factors

The mortality rate of TTP remains 10-20% and after the initial TTP episode, one third of all patients relapse one or multiple times (Joly et al., 2017a; Mancini et al., 2017). Nevertheless, there is only a limited knowledge on factors that can reliably assess the severity of an acute TTP episode and factors that can predict treatment outcome, as well as disease prognosis. Consequently, it is challenging to identify patients that would profit from early treatment intensification or patients that have a high risk of relapsing and might need prophylactic treatment to prevent those relapses (Alwan et al., 2017; Coppo et al., 2019; Yang et al., 2011). Thus, a wider understanding of the prognostic factors of TTP, both directly and indirectly related to TTP pathophysiology, would be of great value. Indicators of poor prognosis that are non-specific to TTP, include increasing age, increased LDH levels, increased cardiac troponin levels and severe neurological involvement (Alwan et al., 2017). Moreover, African Americans have an increased risk of exacerbation (Cataland et al., 2009), although their overall survival

is higher than in Caucasian patients (Martino et al., 2016), indicating that ethnicity is also linked to TTP prognosis. Furthermore, three biomarkers that are directly related to TTP pathophysiology have been studied, namely ADAMTS13 activity, anti-ADAMTS13 autoantibody titer and ADAMTS13 antigen level. Several studies have shown that low ADAMTS13 activity levels, at presentation or during remission, are an indicator of poor prognosis (Cataland et al., 2009; Jin et al., 2013; Kremer Hovinga et al., 2010). In 2006, two groups (Feys et al. and Rieger et al.) found that ADAMTS13 antigen levels were dramatically decreased in iTTP patients in comparison to antigen levels of healthy donors. Consequently, they concluded that the decrease in ADAMTS13 activity in iTTP patients was not only caused by the neutralizing effect of inhibitory anti-ADAMTS13 autoantibodies, but that antigen clearance must also affect ADAMTS13 activity, which was reflected in the low ADAMTS13 antigen levels. In 2017, Alwan et al. found that both low levels of ADAMTS13 antigen and high anti-ADAMTS13 autoantibodies titers were associated with higher mortality. In line with the findings of Feys et al. (2006) and Rieger et al. (2006), they concluded that antigen level, rather than autoantibody titers, was the defining parameter in mortality. This conclusion was based on the finding that ADAMTS13 antigen levels could discriminate between patients that survived and died although they all had high anti-ADAMTS13 IgGs, meaning that a higher antigen level could explain why not all patients with high anti-ADAMTS13 IgGs in the study died (Alwan et al., 2017). This study, which included 312 episodes of 292 patients, reflects the findings of other smaller patient studies performed by Yang et al. in 2011 (40 patients) and by Thomas et al. in 2015 (43 patients) (Thomas et al., 2015; Yang et al., 2011). Yang et al. not only showed that patients with lower antigen level at presentation have a higher chance of dying, they also showed that patients with lower ADAMTS13 antigen level at the initial clinical response have a high propensity to develop TTP exacerbations (Yang et al., 2011). Although, all these studies provide a rationale to include ADAMTS13 antigen levels in the clinical evaluation of TTP patients, ADAMTS13 antigen measurements are not routinely performed.

## 4.4 Therapy

TTP is a medical emergency and when TTP diagnosis is suspected, treatment should be initiated immediately as a delay in treatment could have severe consequences, including severe organ damage and death (Joly et al., 2017a). The mortality rate of TTP decreased from 85-95% to 10-20% when plasma therapy for TTP patients was introduced in the 1970s (Lämmle et al., 2005; Zheng, 2015). The efficacy behind this largely empirical treatment was not well understood, until the discovery of ADAMTS13. This discovery led to a better comprehension of TTP pathophysiology and opened doors to more targeted treatments, including recombinant ADAMTS13. Nonetheless, plasma therapy remains the cornerstone of current TTP management (Coppo et al., 2019). In general, plasma therapy should be maintained until platelet counts and LDH levels normalize, and haemolysis related signs are

ceased. In addition, features related to organ dysfunction should be resolved (Joly et al., 2017a; Knöbl, 2018; Kremer Hovinga et al., 2017).

#### 4.4.1 Congenital TTP

Patients with congenital TTP are treated with plasma infusions to provide sufficient functional ADAMTS13. cTTP patients suffering from recurrent relapses might be treated with prophylactic plasma infusions every two or three weeks, although no official guidelines for prophylactic use have been established (Joly et al., 2017a; Knöbl, 2018; Kremer Hovinga et al., 2017). Plasma therapy, however, exposes the patient to the high risk of pathogen transmission, catheter-related sepsis, cardiac arrest, fluid volume overload and other major complications. Moreover, it is time-consuming and has a serious impact on the quality of life of the patient (George, 2010; Knöbl, 2018; Trionfini et al., 2009). Accordingly, recombinant ADAMTS13 (rADAMTS13) as a prophylactic home-treatment, especially for cTTP patients, has gained a lot of interest in recent years and a phase III clinical trial is in progress (ClinicalTrials.gov NCT03393975) (Coppo et al., 2019; Knöbl, 2018; Kremer Hovinga et al., 2017). However, recombinant protein production is very expensive. As an alternative, gene therapy could be used as a curative therapy considering the underlying genetic defect of cTTP patients (see below 4.4.3).

#### 4.4.2 Immune-mediated TTP

The primary treatment for iTTP patients is plasma exchange (PEX). PEX replaces the patient's plasma with donor plasma to replenish ADAMTS13 and simultaneously remove anti-ADAMTS13 autoantibodies and UL-VWF multimers (Knöbl, 2018; Kremer Hovinga et al., 2017). Plasma infusions should only be performed in these patients when PEX is not immediately available (Knöbl, 2018). In refractory cases or cases with severe organ dysfunction, treatment can be intensified by performing PEX twice daily or by increasing the exchanged plasma volume (Knöbl, 2018). Considering the autoimmune nature of the disease, immunosuppression is also a substantial part in iTTP management. Therefore, corticosteroids are usually co-administered with PEX (Joly et al., 2017b). Corticosteroids, e.g. prednisone, are widely used in autoimmune diseases due to their anti-inflammatory and immunosuppressive attributes. They can pass through the cell membrane and activate intracellular glucocorticoid receptors, which in their turn translocate to the nucleus where they act as transcription factors or interact with other transcription factors to regulate gene expression. Consequently, corticosteroids indirectly reduce the production of cytokines and other inflammatory mediators, inhibit cell migration to sites of inflammation and induce apoptotic cell death in leukocytes (Murphy & Weaver, 2017), thereby also suppressing further anti-ADAMTS13 autoantibody production (Knöbl, 2018). Similarly, rituximab inhibits the production of anti-ADAMTS13 autoantibodies by depleting peripheral B-cells. Rituximab is a humanized anti-CD20 monoclonal antibody that was introduced as a treatment for iTTP patients that are

unresponsive or suffer from disease exacerbation. In addition, rituximab has been used as a prophylactic treatment to prevent relapses in patients that have a persisting or recurring severe ADAMTS13 deficiency during clinical remission or during follow-up (Joly et al., 2017a). Moreover, the high response rates to rituximab in these patients have provided a rationale to administrate it as a frontline-therapy (Joly et al., 2017a; Kremer Hovinga et al., 2017). Finally, although rituximab is very effective in eradicating autoantibodies and outperforms immunomodulators used in the past, the response of the antibody has a delay of approximately two weeks and relapsing of patients is observed after one year (Coppo et al., 2019; Joly et al., 2017b). Alternatively, caplacizumab (ALX-0081) prevents platelet aggregation and activation by binding with high affinity to the VWF A1 domain and thereby competing with platelet receptor GPIIb/IIIa. Caplacizumab is a humanized bivalent nanobody, derived from heavy-chain-only immunoglobulins found in Camelidae. The use of caplacizumab leads to faster recovery of platelet counts and biomarkers for organ damage, as well as less exacerbation. However, caplacizumab does not target the autoimmune response against ADAMTS13 and the relapse rate is high after withdrawal of caplacizumab (Joly et al., 2017a; Knöbl, 2018; Kremer Hovinga et al., 2017; Peyvandi et al., 2016).

In general, ADAMTS13 is the first therapeutic target, then immunosuppressive agents are used to target autoantibodies and finally, drugs are aimed at blocking the binding of VWF to platelets by directly blocking the interaction between VWF and GPIIb/IIIa with caplacizumab or indirectly by reducing the size of the VWF multimers with N-acetylcysteine (Joly et al., 2017b).

**Table 1. Currently used and new strategies for cTTP and iTTP treatment.**

<b>Treatment</b>	<b>Strategy</b>	<b>References</b>
<b>Targeting ADAMTS13</b>		
Plasma Infusion	Replenish ADAMTS13	*
PEX	Replenish ADAMTS13, remove autoantibodies and UL-VWF multimers	*
rADAMTS13	Replenish ADAMTS13	*
<b>Targeting anti-ADAMTS13 autoantibodies</b>		
Corticosteroids	Inhibits autoantibody production (inhibits cytokine production and promotes cell death)	*
Rituximab	B-cell modulation (CD20 <sup>+</sup> cells)	*
Vincristine	B-cell modulation	Blombery & Scully, 2014
Cyclophosphamide	B-cell modulation	Blombery & Scully, 2014
Mycophenolate mofetil	B-cell modulation	Blombery & Scully, 2014
Cyclosporine A	Targets T-cell activation	Joly et al., 2017b
Bortezomib	Targets proteasome	Joly et al., 2017b; Kremer Hovinga et al., 2017
Eculizumab	Targets C5 component of complement system	Joly et al., 2017b
Splenectomy	Knowledge is limited, possibly to remove splenic B-cells that escape other B-cell targeting therapies	Blombery & Scully, 2014; Kremer Hovinga et al., 2017
<b>Targeting the VWF-platelet interaction</b>		
Caplacizumab	Blocks VWF- GPIIb/IIIa interaction	*
N-acetylcysteine	Reduces VWF multimer size	Joly et al., 2017b; Kremer Hovinga et al., 2017

\*References indicated in text above.

### 4.4.3 Gene therapy

Notwithstanding the substantial impact plasma therapy made on the treatment of TTP patients, plasma infusions are expensive and expose the patient to some major complications, including catheter-related sepsis (George, 2010). Therefore, gene therapy might provide an alternative to lifelong treatment with plasma infusions, especially considering that an ADAMTS13 activity of 10% (0.1 µg/mL) is sufficient to protect patients against disease recurrences (Trionfini et al., 2009) and that the underlying genetic defect of cTTP is monogenic. Accordingly, several strategies for cTTP have been tested in *Adamts13*<sup>-/-</sup> mice. These gene delivery strategies comprised of both viral vector systems, including lentiviral (Laje et al., 2009; Niiya et al., 2009), adenoviral (Trionfini et al., 2009) and adeno-associated (Jin et al., 2013) viral vectors, and non-viral approaches, including the *Sleeping Beauty* transposon system (Verhenne et al., 2017) and systemic administration of human ADAMTS13 messenger RNA encapsulated in lipid nanoparticles (Liu-Chen et al., 2018). All these approaches led to the expression of ADAMTS13 or a truncated variant of ADAMTS13 (MDTCS) in *Adamts13*<sup>-/-</sup> mice, which demonstrates the feasibility of gene therapy for cTTP. However, only Jin et al. (2013) and Verhenne et al. (2017) investigated whether the expression of ADAMTS13 protected the mice against TTP development.

*Adamts13*<sup>-/-</sup> mice do not spontaneously develop TTP, even though they show a complete loss of ADAMTS13 activity and have a prothrombotic phenotype (Vanhoorelbeke & De Meyer, 2013). Therefore, a trigger is needed to provoke TTP symptoms, such as a high dose of recombinant human VWF (rVWF) or shigatoxin (Stx). The injection of *Adamts13*<sup>-/-</sup> mice with rVWF, that contains UL-VWF multimers, mimics human TTP as it leads to rapid development of severe thrombocytopenia, schistocytosis, a decrease in haematocrit and increased LDH levels (Schiviz et al., 2012). The relevance of Stx as a trigger of TTP, however, is based on the role that it plays in Stx-associated HUS, also known as typical HUS. Stx-associated HUS is a TMA that is caused by infection with certain bacteria, mainly enterohaemorrhagic *Escherichia coli*, that produce Stx which is toxic to endothelial cells (Kremer Hovinga et al., 2017). Stx-associated HUS can severely affect the kidneys, but also causes bloody diarrhoea, thrombocytopenia, microangiopathic haemolytic anaemia and normal or mildly reduced ADAMTS13 activity (Kremer Hovinga et al., 2017; Motto et al., 2005). Stx only evokes TTP symptoms in *Adamts13*<sup>-/-</sup> mice on a mixed CASA/Rk-C57BL/6J-129X1/SvJ background and not on a C57BL/6J-129X1/SvJ background. This is due to the enhanced susceptibility to the development of TTP signs in *Adamts13*<sup>-/-</sup> mice on a mixed CASA/Rk-C57BL/6J-129X1/SvJ background, caused by the introduction of the genetic background CASA/Rk, a strain that has increased levels of plasma VWF (Motto et al., 2005; Vanhoorelbeke & De Meyer, 2013). *Adamts13*<sup>-/-</sup> mice with this mixed background that are injected with Stx demonstrated severe thrombocytopenia, microangiopathic haemolytic anaemia and widespread microthrombi

formation, and thus also have a phenotype that mimics human TTP (Motto et al., 2005). In the studies performed by Jin et al. (2013) and Verhenne et al. (2017) the *Adamts13<sup>-/-</sup>* mice were challenged with Stx or rVWF, respectively. Triggering of the development of TTP signs was not done in the studies of Niiya et al. (2009), Laje et al. (2009), Trionfini et al. (2009) and Liu-Chen et al. (2018). Additionally, it remains questionable whether these gene delivery methods, administered via *in utero* injection (Niiya et al., 2009) or via tail vein injections (Jin et al., 2013; Laje et al., 2009; Liu-Chen et al., 2018; Trionfini et al., 2009; Verhenne et al., 2017), can be translated to gene therapy methods for humans. Therefore, more in-depth research focussing on clinically relevant gene therapy strategies is needed, e.g. using intramuscular electrotransfer (André & Mir, 2004) to introduce the naked plasmid DNA in the muscle cells of *Adamts13<sup>-/-</sup>* mice.

A disadvantage of plasmid DNA is that it can be lost when the cell undergoes mitosis due to the episomal state of the plasmid DNA (Hollevoet & Declerck, 2017). However, differentiated skeletal muscle cells are non-mitotic and can therefore result in long-term expression of the delivered gene (Hollevoet & Declerck, 2017). The main advantage of plasmid DNA is that it allows for easy molecular cloning and it presents less concerns in terms of biosafety compared to viral vectors as it has a decreased risk of genotoxicity, a major complication when using lentiviral vectors, and it has a low immunogenicity, which is a major disadvantage when working with adenoviral vectors (André & Mir, 2004; Hollevoet & Declerck, 2017; Trionfini et al., 2009).

However, the *in vivo* gene expression, independently of the gene delivery method, can still evoke an anti-drug antibody (ADA) response. This ADA response can even be substantially higher than would be evoked by protein administration (Hollevoet, De Smidt, Geukens, & Declerck, 2018). Thus, although the immunogenicity of ADAMTS13 is most likely low, which can be concluded from the fact that only a few cases have been reported regarding alloantibody formation against plasma-derived ADAMTS13 in cTTP (Raval et al., 2015), the humoral response in *Adamts13<sup>-/-</sup>* mice against the *in vivo* expressed ADAMTS13 could still present some complications (Kremer Hovinga & Voorberg, 2012). Therefore, if one would like to use a DNA-based delivery system to express ADAMTS13 in mice, two routes should be pursued to analyse the *in vivo* ADAMTS13 expression (Hollevoet et al., 2018). To assess whether the protein is expressed successfully using the designed plasmid system, ADAMTS13 gene transfer should be evaluated in immune-compromised mice. To analyse the actual ADA response, the gene transfer should be evaluated in immune-competent mice. This has to be done because it is important to verify whether the system can lead to expression of ADAMTS13, but it is also important to know whether long-term expression in a clinically relevant model can be accomplished, or at least whether repeated dosing is tolerated in this model (Hollevoet et al., 2018).

Thus, to investigate new DNA-based gene therapy strategies, both *Adamts13*<sup>-/-</sup> mice and immunodeficient *Adamts13*<sup>-/-</sup> mice, such as *Adamts13*<sup>-/-</sup>*Rag1*<sup>tm1Mom/tm1Mom</sup> mice, are needed. RAG1 and RAG2, encoded by the recombination activating genes 1 and 2 (*RAG1* and *RAG2*), form a dimer that initiates V(D)J recombination in early T- and B-cell development. In this process different gene segments are recombined that will encode the T-cell and B-cell receptors. B-cell receptors are composed of a membrane-bound immunoglobulin that has a certain antigen specificity. When the B-cell is activated and differentiates into a plasma B-cell, it will produce antibodies with that same antigen specificity as the B-cell receptor (Murphy & Weaver, 2017). Mice homozygous for the *Rag1*<sup>tm1Mom</sup> mutation do not produce mature B- and T- lymphocytes as lymphocyte differentiation arrests at an early stage due to the inability to perform V(D)J recombination (Mombaerts et al., 1992).

# Chapter 5

## Objectives

The first part of this thesis focuses on three enzyme-linked immunosorbent assays (ELISAs) that measure three critical ADAMTS13 markers: ADAMTS13 activity, anti-ADAMTS13 autoantibodies and ADAMTS13 antigen. The second part focuses on the development of a clinically relevant gene therapy approach for cTTP.

## Diagnosis and prognosis

One of the challenges of TTP management is the complex diagnosis due to the rarity of the disease, the diversity of the clinical signs and symptoms and the overlap of these signs and symptoms with other TMAs. Moreover, the essential information concerning ADAMTS13 activity is mostly not readily available, but given the emergency setting of an acute TTP episode, treatment is already initiated when TTP is suspected based on the clinical signs and symptoms rather than the conclusive diagnosis based on ADAMTS13 measurements. Nonetheless, measurement of the ADAMTS13 activity level plays a pivotal role in the diagnostic process of a TTP patient, as ADAMTS13 activity below 10% is the only specific biomarker for TTP, and thus the only diagnostic feature that can confirm TTP. ADAMTS13 activity levels can be measured using fluorescence resonance energy transfer (FRET) assays, such as FRETs-VWF73 (Kokame et al., 2005) and FRETs-rVWF71 (Muia et al., 2013), which are well-established in expert laboratories. However, the fluorogenic substrates used in these assays are extremely expensive and patented (US8663912B2, 2014) and the assay requires considerable technical expertise and costly equipment to measure fluorescence, all major disadvantages in a clinical, as well as a research setting. ADAMTS13 activity can also be measured using the TECHNOZYM ADAMTS-13 Activity ELISA (Technoclone, Vienna, Austria). However, this assay is again high-priced and the method used to determine ADAMTS13 activity in this assay and antibodies that can recognize cleaved VWF in general, are patented (EP1852442B1, 2012). For that reason, the first part of this project focusses on the adaptation of the VWF96 ADAMTS13 activity ELISA for the use of citrated human plasma (**AIM 1**), to obtain an in-house developed ADAMTS13 activity test, as this test was previously developed for the use of recombinant ADAMTS13 (Schelpe, 2018). This was done in collaboration with Dr. J. Crawley (Centre for Haematology, Imperial College London, London, United Kingdom) who kindly provided the VWF96 substrate. Another part of the diagnostic procedure of TTP is the measurement of anti-ADAMTS13 autoantibodies, along with *ADAMTS13* gene sequencing, to distinguish between the two major forms of TTP: cTTP and iTTP. In the Laboratory for Thrombosis Research, the anti-ADAMTS13 autoantibody titers can

be determined using the in-house anti-ADAMTS13 autoantibody ELISA. As a part of the characterisation process of the in-house anti-ADAMTS13 autoantibody ELISA, a reliable cut-off that discriminates between individuals with and without anti-ADAMTS13 autoantibodies was established (**AIM 2**).

A second challenge in managing TTP is the limited knowledge about prognostic factors that can identify TTP patients that would profit from early treatment intensification or are at high risk of relapsing. Studies have shown that a reduced ADAMTS13 antigen level, in addition to reduced ADAMTS13 activity and high anti-ADAMTS13 autoantibody titers, is an extremely valuable biomarker of poor prognosis. Nevertheless, ADAMTS13 antigen levels are not included in the standard diagnostic tests for TTP patients. The ADAMTS13 antigen levels of a large cohort of samples, including 424 healthy donor and 19 iTTP patient plasma samples, were measured to characterise the in-house ADAMTS13 antigen ELISA (**AIM 3**).

## Gene therapy

Plasma infusions are used to treat cTTP patients, when they experience an acute TTP episode, to provide them with sufficient functional ADAMTS13. However, 40% of the cTTP patients suffer from recurring episodes and receive prophylactic plasma infusions every two or three weeks. Notwithstanding the substantial impact plasma therapy made on the treatment of TTP patients, plasma infusions are expensive, time-consuming and exposes the patient to some major complications, including catheter-related sepsis. As an alternative, gene therapy for cTTP patients as the expression of functional ADAMTS13 could compensated the need for plasma infusions. Considering the underlying genetic defect of cTTP, gene therapy might be an alternative treatment option for cTTP patients as the expression of functional ADAMTS13 could compensated the need for plasma infusions. A variety of gene therapy approaches have been tested in preclinical mouse models and demonstrate the feasibility of gene therapy for cTTP. However, strategies focusing on clinically relevant gene delivery methods are needed. Here, an alternative gene therapy strategy is initiated that would introduce the *ADAMTS13* gene into muscle cells using intramuscular electrotransfer, a well-established technique in humans. Therefore, a plasmid was created containing the murine *ADAMTS13* gene and the CAG promotor and gene expression was verified *in vitro* in a murine myoblast cell line (**AIM 4**).

**Part II**

**Materials & Methods**

# Chapter 6

## Diagnosis and prognosis

### 6.1 Plasma Samples

Citrated plasma samples from 424 healthy donors (HDs) and 19 acute iTTP patients were available for analysis. The HD samples were kindly provided by the Belgian Red Cross-Flanders (Ghent, Belgium) and the iTTP patient samples by the Aix-Marseille Université (Marseille, France). Analyses were approved by the local Ethical Committees and informed consent was obtained in accordance with the Declaration of Helsinki. Specified product information and buffer compositions can be found in the addendum (Addendum II and Addendum III).

### 6.2 Human ADAMTS13 activity ELISA

The VWF96 ADAMTS13 activity ELISA measures the proteolytic activity of ADAMTS13 under static conditions. These static conditions cannot induce the unfolding of the VWF A2 domain needed for proteolysis of the VWF Y1605 - M1606 peptide bond. Therefore, VWF96, kindly provided by Dr. J. Crawley (Centre for Haematology, Imperial College London, London, United Kingdom), is used as a functional substrate for ADAMTS13. VWF96 is a short recombinant oligopeptide consisting of 96 amino acid residues of the VWF A2 domain (G1573-R1668) including the Y1605 - M1606 peptide bond. The VWF96 substrate also contains an N-terminal HisG tag (HHHHHHG) and a C-terminal herpes simplex virus (HSV) tag (QPELAPEDPED). The VWF96 ADAMTS13 activity ELISA, as previously described with recombinant ADAMTS13 (Schelpe, 2018), was adapted for the use of citrated human plasma (Figure 9). The monoclonal murine anti-HisG antibody (diluted 1/1000) was coated on a 96-well microtiter plate in carbonate/bicarbonate buffer (Table AIII.1) and incubated overnight (ON) at 4°C in a wet chamber. Next, the plate was washed three times with Phosphate Buffered Saline (PBS; Table AIII.2) with 0.1% Tween20 and blocked with 3% dried milk powder in PBS for two hours at room temperature (RT). Then, the microtiter plate was again washed three times with PBS/0.1% Tween20 and incubated for one hour with VWF96 (140 nM in PBS/0.3% milk). The N-terminal HisG tag of VWF96 is recognized and bound by the coated anti-HisG antibody. After incubation, the plate was washed six times in PBS/0.1% Tween20. Normal human plasma (NHP) was thawed at 37°C for five minutes before use and NHP was added to the plate in a dilution series using the appropriate activity buffer. Several buffers were tested, based on activity buffers used in other ADAMTS13 activity assays, namely the HEPES-buffered saline (HBS) solution used by De Cock et al. (2015), the Bis-Tris buffer used by

Kokame et al. (2005) and the acetate buffer used by Kato et al. (2006). As mentioned, the exact buffer compositions can be found in the addendum (Addendum III). NHP (starting dilution 1/4 or 1/10 for the HBS and Bis-Tris buffer or the acetate buffer, respectively) was added to the plate in a 1.5 over 2.5 dilution series (for the HBS and Bis-Tris buffer) or in a 1 over 2 dilution series (for the acetate buffer) and incubated at 37°C for one hour. Then, the plate was washed six times and polyclonal goat anti-HSV antibodies conjugated to horseradish peroxidase (HRP) (diluted 1/2000 in PBS/0.3% milk) were added to the wells and incubated for one hour at RT. These anti-HSV antibodies recognized the C-terminal HSV tag of the VWF96 substrate. After incubation, the plate was washed six times. Next, the colouring solution (Table 2) with *o*-phenylenediamine dihydrochloride (OPD) and hydrogen peroxide (H<sub>2</sub>O<sub>2</sub>) in phosphate buffer and citric acid buffer was added to the plate. The colouring reaction was stopped with 4 M sulfuric acid (H<sub>2</sub>SO<sub>4</sub>). Finally, the optical density (OD) was determined at 492 and 630 nm with the FLUOstar Omega microplate reader. High ADAMTS13 activity, and thus high proteolysis of VWF96, results in low OD values (Figure 9 A). Accordingly, low ADAMTS13 activity results in high OD values (Figure 9 B). The average OD value of four coated wells incubated with VWF96 but where solely activity buffer was added was set to 1 to calculate relative OD values. The ADAMTS13 activity levels of undiluted NHP was set to 100%.

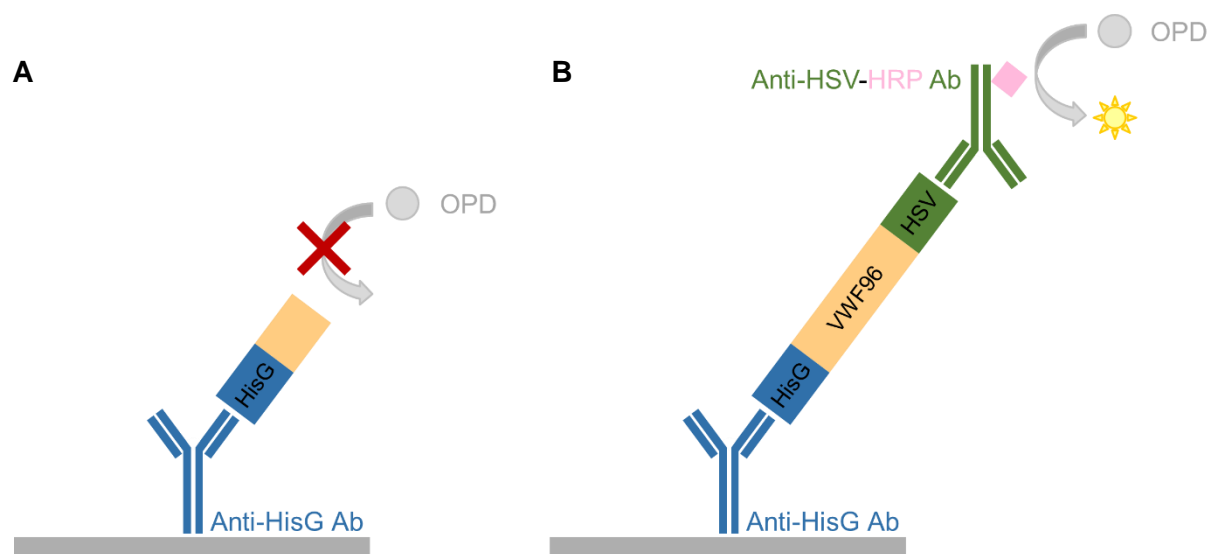


**Figure 9. Experimental set-up of the ADAMTS13 activity ELISA.** An ELISA plate was coated with anti-HisG antibody. Then, VWF96 fused with an N-terminal HisG-tag and a C-terminal HSV-tag was added. Next, NHP containing human ADAMTS13 was added and eventually anti-HSV antibody conjugated to HRP. Finally, the colouring reaction was performed with OPD and H<sub>2</sub>O<sub>2</sub> in phosphate buffer and citric acid buffer and the absorbance was measured at 492 and 630 nm. (A) When ADAMTS13 activity in the well is high, a higher amount of VWF96 will be proteolyzed. When VWF96 is cleaved, the anti-HSV antibody is not able to bind and a low OD value is expected. (B) When ADAMTS13 activity in the well is low. Only a small amount of VWF96 will be proteolyzed and the anti-HSV antibody can bind to the HSV tag. Subsequently, HRP will be able to catalyse the colouring reaction with OPD and H<sub>2</sub>O<sub>2</sub>. This results in a higher OD value.

## 6.3 Human anti-ADAMTS13 autoantibody ELISA

Anti-ADAMTS13 autoantibody titers were determined for all HD and iTTP patient plasma samples as previously described (Roose, 2018b; Schelpe et al., 2018), with major modifications (Figure 10). Recombinant human ADAMTS13 (rhADAMTS13; 15 nM in PBS) was coated on a 96-well microtiter plate and incubated ON at 4°C. The HD and iTTP patient samples were thawed at 37°C before use. After blocking, a 1/40 dilution of the samples in PBS/0.3% milk was added to the plate and incubated for one hour at 37°C. After incubation, polyclonal goat anti-human IgG (Fc specific) antibodies conjugated to HRP (diluted 1/10 000 in PBS/0.3% milk) was added and incubated for one hour at RT. Then, the colouring reaction was performed and stopped with H<sub>2</sub>SO<sub>4</sub> after ten minutes. The OD was determined at 492 and 630 nm with the FLUOstar Omega reader. The blocking step, washing steps and colouring reaction were performed as described above. A high titer iTTP plasma sample was set to 100% and used as a reference to calculate the anti-ADAMTS13 autoantibody titers of the samples. Therefore, the high titer sample (starting dilution 1/80) was added to the plate in a 1 over 2 dilution series in PBS/0.3% milk. As a negative control, each HD and iTTP sample was also added to a non-coated well on the plate in a 1/40 dilution in PBS/0.3% milk. HD samples with an OD-value higher than 0.1 for the non-coated well were excluded. Then, the anti-ADAMTS13 autoantibody titers of 404 HD samples were used to establish the cut-off value of the assay by determining the 97.5th percentile.

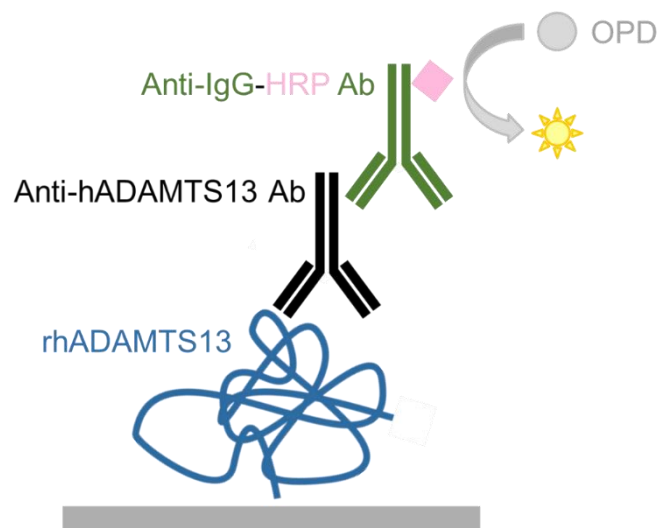


**Figure 10. Experimental set-up of the human anti-ADAMTS13 autoantibody ELISA.** An ELISA plate was coated with rhADAMTS13. Next, plasma samples with human anti-ADAMTS13 autoantibodies were added. Then, anti-human IgG (Fc specific) antibody conjugated to HRP was added. The colouring reaction was performed with OPD and H<sub>2</sub>O<sub>2</sub> in phosphate buffer and citric acid buffer and the absorbance will be determined at 492 and 630 nm.

## 6.4 Human ADAMTS13 antigen binding ELISA

Human ADAMTS13 (hADAMTS13) antigen levels were measured for all HD and iTTP patient plasma samples as previously described (Alwan et al., 2017; Schelpe et al., 2018), with minor modifications (Figure 11). A 96-well microtiter plate was coated with in-house developed monoclonal murine anti-hADAMTS13 antibody 3H9 (5 µg/mL in carbonate/bicarbonate buffer) and incubated ON at 4°C. The plasma samples were thawed at 37°C for five minutes before use. After blocking, the plasma samples (starting dilution of 1/100 or 1/12.5 for HD and iTTP patient samples, respectively) were added in a 1.5 over 2.5 dilution series in PBS/0.3% milk and incubated for 1.5 hours at 37°C. Then, a mix of in-house developed biotinylated monoclonal murine anti-hADAMTS13 antibodies 19H4 and 17G2 (1.5 µg/mL each in PBS/0.3% milk) was added to each well and the plate was incubated for one hour at RT. Next, HRP-labelled streptavidin (1/10 000 dilution in PBS/0.3% milk) was added. After an incubation of one hour at RT, the colouring reaction was performed and stopped with H<sub>2</sub>SO<sub>4</sub> after exactly ten minutes. Finally, absorbance was measured at 490 and 650 nm with the FLUOstar OPTIMA reader. The blocking step, washing steps and colouring reaction were performed as described above. Afterwards, a reference curve was made to calculate ADAMTS13 antigen concentrations using NHP that was added to the plate in duplicate in a 1.5 over 2.5 dilution series in PBS/0.3% milk (starting dilution 1/70) and was set to 1 U/mL ADAMTS13 antigen. NHP was also added in a 1.5 over 2.5 dilution series with a starting dilution of 1/100, as an internal control.

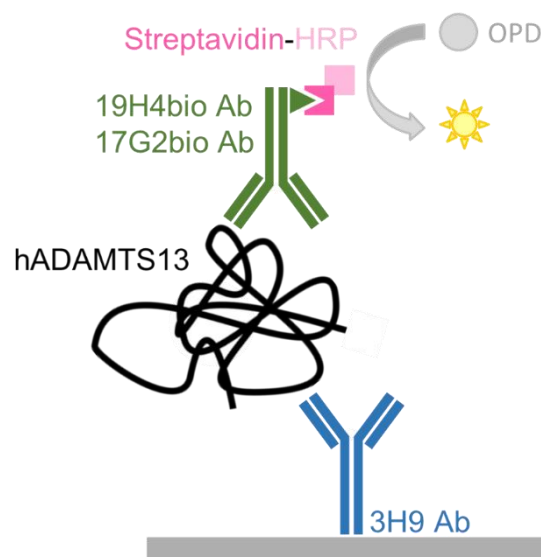


**Figure 11. Experimental set-up of the human ADAMTS13 antigen binding ELISA.** An ELISA plate was coated with anti-hADAMTS13 (3H9) antibody. Next, plasma samples with human ADAMTS13 were added. Then, bound ADAMTS13 was detected with biotinylated anti-hADAMTS13 (19H4 and 17G2) antibodies, followed by HRP-labelled streptavidin. Finally, the colouring reaction was performed with OPD and H<sub>2</sub>O<sub>2</sub> in phosphate buffer and citric acid buffer and the absorbance was determined at 490 and 650 nm.

**Table 2. Composition of colouring solution (per 96-well microtiter plate).**

<b>Product</b>	<b>Supplier</b>	<b>Cat. Number</b>
10 mL phosphate buffer: 0.1 M Na <sub>2</sub> HPO <sub>4</sub> ·2H <sub>2</sub> O	Sigma	71643
10 mL citric acid buffer: 0.05 M citric acid	Sigma	124910010
8 µL H <sub>2</sub> O <sub>2</sub> (35%)	Acros Organics	202065000
200 µL OPD (50 g/L*)	Sigma	P1526

\*Note: OPD is diluted to 50 g/L in 50% phosphate buffer and 50% citric acid buffer.

# Chapter 7

## Gene therapy

*In vitro* experiments were performed in collaboration with G. Vermeire (Laboratory for therapeutic and diagnostic antibodies, KU Leuven). Specified product information and buffer compositions can be found in the addendum (Addendum II and Addendum III)

### 7.1 Construction of the pMA-CAG-mADAMTS13 plasmid

The most important components of the constructed pMA-CAG-mADAMTS13 plasmid are the murine *ADAMTS13* (*mADAMTS13*) gene under control of the cytomegalovirus immediate-early enhancer-chicken- $\beta$ -actin hybrid (CAG) promoter, a pUC-type bacterial origin of replication and an ampicillin resistance gene. The CAG promoter is a general promoter with high activity in the muscles (Aihara & Miyazaki, 1998). This plasmid was generated from the pBS-II-SK-HCHRPi-mADAMTS13 vector (Figure 12) (available in the Laboratory for Thrombosis Research) and the pMA-CAG-TMab2\_LC#9 vector (Figure 13) (kindly provided by prof. Paul Declerck, Laboratory for therapeutic and diagnostic antibodies, KU Leuven) using the In-Fusion® HD Cloning Kit (Figure 14). The In-Fusion HD enzyme can very efficiently and precisely fuse polymerase chain reaction (PCR) generated inserts and linearized vectors that have 15 bp overlaps.

First, the pMA-CAG-TMab2\_LC#9 vector was linearized (Figure 14 Step 1) using two restriction enzymes, *AgeI* and *BstBI*, in two sequential steps due to a difference in optimal incubation temperatures (37°C and 65°C, respectively) as instructed by the supplier. After the first digestion with *AgeI*, the digestion product was purified using the NucleoSpin Gel and PCR Clean-up kit following the “PCR clean-up” protocol given by the manufacturer. This kit uses a spin-column purification technology: it binds DNA fragments to a silica-membrane, washes away the undesired products and then elutes the purified DNA. After the purification, the second digestion was performed with *BstBI*.

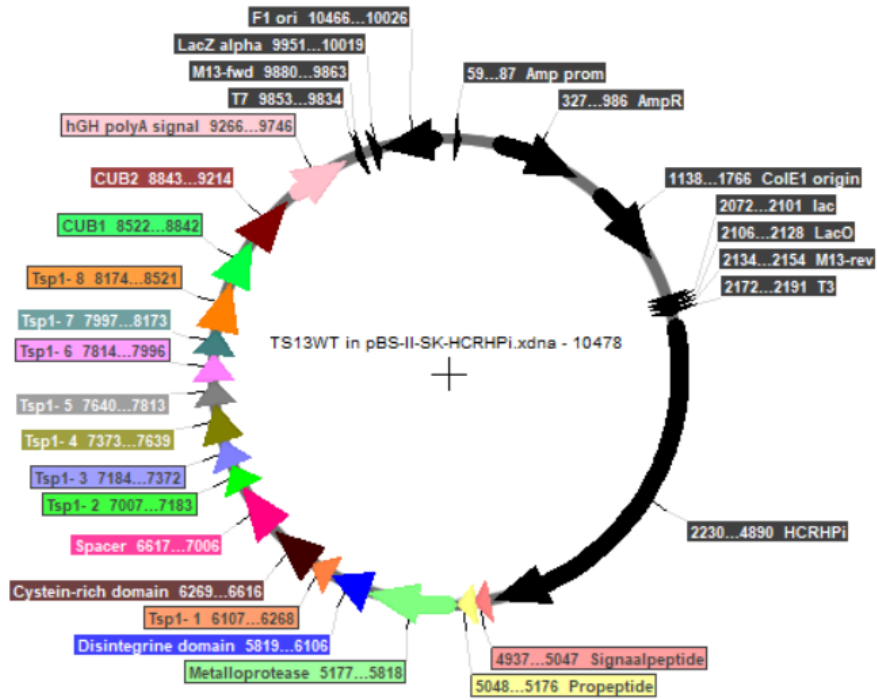


Figure 12. Vector map of pBS-II-SK-HCRHPI-mADAMTS13.

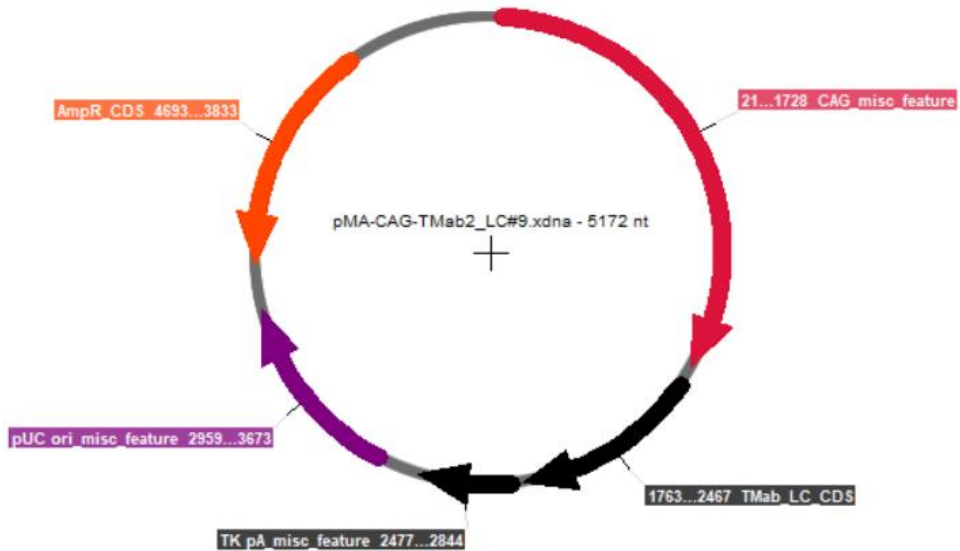
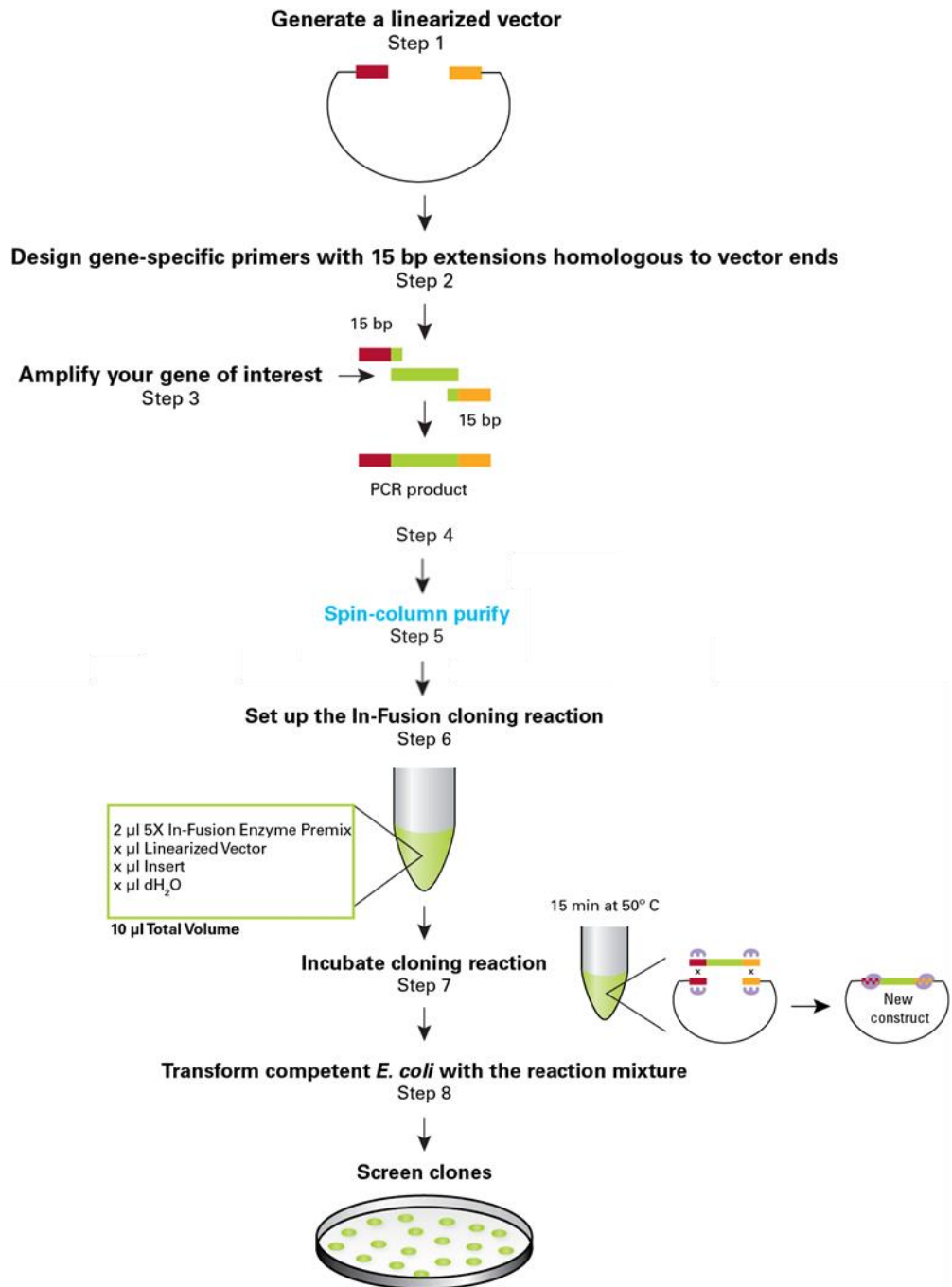


Figure 13. Vector map of pMA-CAG-TMab2\_LC#9 vector.



**Figure 14. Construction of the plasmid In-Fusion® HD Cloning Kit .** The vector, used as a bacterial backbone, was linearized (Step 1). Gene-specific primers were designed with 15 bases at the 5' end that are homologous to the linearized vector ends (Step 2). The insert was amplified via PCR using the designed primers (Step 3). The PCR product (and linearized vector) were verified via gel electrophoresis (Step 4). Next, the DNA fragments were purified using spin-column purification technology (Step 5). The cloning reaction was set up and performed using the In-Fusion HD Enzyme Premix (Step 6 and 7). Then, *Escherichia coli* cells were transformed with the reaction mixture to amplify the constructed plasmid (Step 8). Afterwards, the cells were spread on LB agar plates containing an antibiotic appropriate for the cloning vector to screen the clones.

Secondly, forward and reverse primers were designed to amplify the DNA fragment encoding mADAMTS13 (Figure 14 Step 2). The 3' end of the primers was specific to the regions flanking the mADAMTS13 DNA fragment in the pBS-II-SK-HCHRPi-mADAMTS13 vector and the 5' end of the primers contained 15 bases homologous to the ends of the linearized pMA-CAG-TMab2\_LC#9 vector. Subsequently, the mADAMTS13 DNA fragment was amplified from the pBS-II-SK-HCHRPi-mADAMTS13 vector following the PCR protocol provided with the Phusion® High-Fidelity DNA Polymerase using the designed primers (Figure 14 Step 3; Table 3).

**Table 3. PCR conditions for amplification of mADAMTS13 gene from the pBS-II-SK-HCHRPi-mADAMTS13 vector using the Phusion® High-Fidelity DNA Polymerase.**

<b>Forward primer</b>	5' CTTCTTTTCGCCTTCGGGGATCCTCTAGAGTCGAAGG 3'
<b>Reverse primer</b>	5' AGCGGAACGGACCGGCCGCACGTGGTTACCTACAAA 3'
<b>Initial denaturation</b>	98°C (1 min)
<b>Denature</b>	98°C (15 s)
<b>30 PCR cycles</b>	
<b>Anneal</b>	59°C (30 s)
<b>Extend</b>	72°C (2 min 40 s)
<b>Final Extension</b>	72°C (10 min)

Then, the linearized vector and the mADAMTS13 PCR product were verified via gel electrophoresis on a 1% agarose gel (Figure 14 Step 4; Table 4). Next, the DNA fragments were excised from the gel and purified according to the “DNA extraction from agarose gels” protocol again provided with the NucleoSpin Gel and PCR Clean-up kit (Figure 14 Step 5). Thereafter, the concentrations of the purified linearized vector and the purified mADAMTS13 PCR product were estimated, which is important for the subsequent cloning, by running 5 µL of each on a 1% agarose gel and using a 1 kb ladder as a reference.

**Table 4. Composition of 1%, 1.5% and 1.8% agarose gel (80 mL).**

<b>Product</b>	<b>Supplier</b>	<b>Cat. Number</b>
44.5 mM Tris	Sigma	252859
44.5 mM boric acid	Acros Organics	217085000
1 mM Na <sub>2</sub> EDTA	Fisher Bioreagents	BP120-500
1% = 0.1 mg; 1.5% = 1.2 mg; 1.8% = 1.44 mg of Ultrapure agarose	Invitrogen	16500-100
8 µL GelGreen: 10000x	VWR	41004

Note: To each sample 1/6 volume of 6X DNA Loading Dye (0.25% bromophenol blue, 40% sucrose, in MilliQ) was added.

Next, the cloning reaction was performed (Figure 14 Step 6 and 7) using the “In-Fusion Cloning Procedure for Spin-Column Purified PCR Fragments” protocol with an insert to vector ratio of 1:1 (both at 3 ng/μL). Subsequently, NovaBlue cells made chemically competent in-house were transformed with the reaction mixture for amplification of the constructed plasmid (Figure 14 Step 8). Briefly, 2 μL of plasmid DNA was added to 50 μL of cells and incubated for 30 minutes on ice. Next, a heat-shock of 30 seconds at 42°C was applied to the cells and the cells were incubated on ice for 2 minutes. This sudden increase in temperature enhanced the DNA passage by creating a thermal imbalance that forced the DNA molecules into the cells. Then, 200 μL of Super Optimal broth with Catabolite repression medium was added and incubated for 1h at 37°C on a shaker, which allows the culture to grow. Afterwards, the cells were plated on ampicillin (50 μg/mL) selective LB agar plates and incubated ON at 37°C to grow the clones. After incubation, the plasmid DNA was isolated from twelve distinctive colonies using the QIAprep Spin Miniprep Kit following the protocol provided by the manufacturer, with minor modifications. First, twelve colonies were picked from the agar plates and grown ON in 3 mL of ampicillin selective LB medium. Secondly, the ON cultures were centrifuged for five minutes at 4000 rpm to form a pellet of the bacterial cells. Thirdly, the cells were resuspended, lysed with the provided buffers and transferred to a spin column. By creating the appropriate conditions in the spin column, the silica-membrane in the spin column separates the DNA from other organic material. After several washing step, high-purity plasmid DNA could be eluted from the spin column.

Thereafter, the presence of the *mADAMTS13* gene in the purified plasmid DNA of all twelve colonies was analysed according to the PCR protocol provided with The Platinum™ SuperFi™ DNA Polymerase with forward primer, mTS13F2, and reverse primer, mTS13R2 (Table 5). After PCR, the PCR products were verified via gel electrophoresis on a 1.5% agarose gel (Table 4) and three plasmids containing the *mADAMTS13* DNA fragment were sent to LGC Genomics (Berlin, Germany) to check the orientation of the *mADAMTS13* gene via sequencing. Then, one of the three plasmids was selected for full sequencing (LGC genomics) of the *mADAMTS13* gene, and subsequent *in vitro* testing.

**Table 5. PCR conditions for PCR screening of purified plasmid DNA of all twelve colonies using the Platinum™ SuperFi™ DNA Polymerase.**

<b>Forward primer</b>	mTS13 F2 5' CTGGAGCCCAAGGATGTG 3'
<b>Reverse primer</b>	mTS13 R2 5' CAGCCCCAGAACCGAAAG 3'
<b>Initial denaturation</b>	98°C (30 s)
<b>Denature</b>	98°C (10 s)
<b>30 PCR cycles</b>	<b>Anneal</b> 52°C (10 s)
	<b>Extend</b> 72°C (30 s)
<b>Final Extension</b>	72°C (5 min)

## 7.2 *In vitro* testing of the pMA-CAG-mADAMTS13 plasmid

C2C12 murine myoblasts (7500 cells per well), were seeded in dulbecco's modified eagle medium with 10% fetal bovine serum on a 96-well microtiter plate. Then, the selected pMA-CAG-mADAMTS13 plasmid (0.1µg/200 µL medium) and X-tremeGENE™ HP DNA Transfection Reagent (0.3 µg/200 µL medium) were added. Certain components of the transfection reagent formed a complex with the plasmid DNA, and then the complex was transported into the cells. Five days after the transfection, the supernatant of each well was collected and frozen at -80°C until the transgene expression could be evaluated via the murine ADAMTS13 (mADAMTS13) antigen ELISA as previously described (De Cock et al., 2015; Deforche et al., 2016) (Figure 15). Therefore, a 96-well microtiter plate was coated with an in-house developed monoclonal murine anti-mADAMTS13 antibody 14H7B8 (5 µg/mL in carbonate/bicarbonate buffer) and incubated ON at 4°C. The supernatant samples obtained from the *in vitro* experiment were thawed at 37°C for five minutes. After blocking, the samples (starting dilution of 1/2) were added in a 1 over 2 dilution series in PBS/0.3% milk and incubated for 1.5 hours at 37°C. Then, in-house produced polyclonal rabbit anti-mADAMTS13 antibodies (5 µg/mL in PBS/0.3% milk) were added to the plate and incubated for one hour at RT. Next, the plate was incubated with polyclonal HRP-labelled goat anti-rabbit IgG antibodies (diluted 1/10 000 in PBS/0.3% milk) for one hour at RT. The blocking step, washing steps and colouring reaction were performed as described above. Afterwards, absorbance was measured at 490 and 650 nm with the FLUOstar OPTIMA reader. The OD value of normal murine plasma (NMP) (1/80 dilution) was used as a reference and set to 1 to calculated relative OD values. Therefore, NMP was added to the plate in a 1/80 dilution in PBS/0.3% milk. As a negative control, supernatant of non-transfected cells was used.

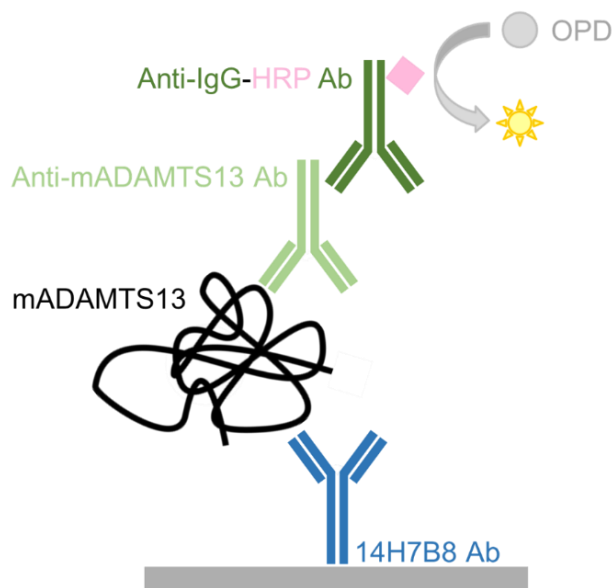


**Figure 15. Experimental set-up of the murine ADAMTS13 antigen binding ELISA.** An ELISA plate was coated with anti-mADAMTS13 antibody (14H7B8). Next, supernatant samples containing secreted mADAMTS13 were added. Then, rabbit anti-mADAMTS13 antibodies were added, followed by HRP-labelled goat anti-rabbit IgG antibodies. Finally, the colouring reaction was performed with OPD and H<sub>2</sub>O<sub>2</sub> in phosphate buffer and citric acid buffer and the absorbance was determined at 490 and 650 nm.

### 7.3 Preparation of the pMA-CAG-mADAMTS13 plasmid

The pMA-CAG-mADAMTS13 plasmid will be used for *in vivo* experiments in the near future. The plasmid will be introduced into the muscle cells of *Adamts13* knockout mice via intramuscular electrotransfer. Therefore, the pMA-CAG-mADAMTS13 plasmid was produced in large quantities and purified following the protocol provided with the EndoFree Plasmid Mega Kit, with minor modifications. Briefly, Novablue cells were transformed with the plasmid (as described above) and a single colony was picked from the agar plates and grown in 3 mL of ampicillin selective LB medium. Then, the cultures were diluted to 1/1000 into 500 mL selective LB medium and grown ON at 37°C. Next, the ON culture was harvested by centrifuging at 6000 rpm for 15 min at 4°C. Using the buffers provided with the kit, the cells were resuspended and lysed, and the genomic DNA was precipitated along with proteins, cell debris, etc. Then, the lysate was transferred to the QIAfilter Mega-Giga Cartridge that clears the lysate and removes endotoxins, when the appropriate conditions are created. The cleared lysate was loaded onto the QIAGEN-tip 2500 which uses an anion-exchange technology to selectively bind plasmid DNA, again under the appropriate conditions, and removes RNA, proteins, and other impurities. The purified plasmid DNA was then eluted, desalted by isopropanol

precipitation and collected in a pellet by centrifuging for 60 min at 4500 rpm at 4°C. Then, the DNA pellet was washed with ethanol and dissolved in the provided endotoxin-free buffer.

## 7.4 Creation of immunodeficient *Adamts13* knockout mice

*Adamts13*<sup>-/-</sup> mice with a mixed CASA/Rk-C57BL/6J-129X1/SvJ background were crossed with RAG1-deficient mice (JAX stock #002216; Mombaerts et al., 1992), homozygous for the *Rag1*<sup>tm1Mom</sup> mutation, with a C57BL/6J background to generate *Adamts13*<sup>-/-</sup>*Rag1*<sup>tm1Mom/tm1Mom</sup> mice. *Adamts13*<sup>-/-</sup> mice do not produce functional ADAMTS13, due to the deletion of exon 1 to 6 of the *mADAMTS13* gene, including the translation start site, the SP region, the P region and most of the M domain (Motto et al., 2005). A 1356 bp deletion in the 5' end of the coding sequence of *RAG1*, which includes the nuclear localization signal and the zinc finger-like motif, results in the mutated *RAG1* gene (*Rag1*<sup>tm1Mom</sup>) (Mombaerts et al., 1992). Ear tissue, obtained via ear punch biopsies, was used to genotype the offspring. Therefore, the genomic DNA was extracted from the ear tissue using the HotSHOT method as described (Truett et al., 2000), with minor modifications. This is a simple, inexpensive and rapid method to prepare PCR-quality genomic DNA using an alkaline sodium hydroxide (NaOH) solution (Table AIII.6) to lyse the cells and using Tris solution (Table AIII.7) as a pH neutralizing reagent. Briefly, 75 µL NaOH solution was added to the ear tissue samples and incubated for 10 min at 95°C while shaking the samples at 1400 rpm. Then, the samples were incubated for 10 min at 4°C. Next, 75 µL Tris solution was added. The samples were then either stored at -20°C or immediately used for subsequent PCR. The PCR-based genotyping of both the *ADAMTS13* and *RAG1* gene was performed according to the protocol provided with the Platinum™ Taq DNA Polymerase using a primer set to amplify the wild type (WT) allele and a different primer set for the mutated allele (Table 6 and 7). For each PCR reaction, 20 µL was run on a 1.8% agarose gel (Table 4).

**Table 6. PCR conditions for ADAMTS13 genotyping using the Platinum™ Taq DNA Polymerase.**

<b>Primer set WT allele</b>	<b>Forward</b>	5' TGGTTCTAAGTACTGTGGTTTCCA 3'
	<b>Reverse</b>	5' GAGTTGCTAGGTTATCAGGAAGGA 3'
<b>Primer set mutated allele</b>	<b>Forward</b>	5' AGCCCCAACTCTTGTCTTTTAAT 3'
	<b>Reverse</b>	5' GAGTTGCTAGGTTATCAGGAAGGA 3'
<b>Initial denaturation</b>		95°C (2 min)
<b>30 PCR cycles</b>	<b>Denature</b>	95°C (30 s)
	<b>Anneal</b>	56°C (30 s)
	<b>Extend</b>	72°C (1 min)
	<b>Final Extension</b>	72°C (10 min)

**Table 7. PCR conditions for RAG1 genotyping using the Platinum™ Taq DNA Polymerase.**

<b>Primer set WT allele</b>	<b>Forward</b>	5' TCTGGACTTGCCTCCTCTGT 3'
	<b>Reverse</b>	5' CATTCCATCGCAAGACTCCT 3'
<b>Primer set mutated allele</b>	<b>Forward</b>	5' TGGATGTGGAATGTGTGCGAG 3'
	<b>Reverse</b>	5' CATTCCATCGCAAGACTCCT 3'
<b>Initial denaturation</b>		95°C (2 min)
<b>Denature</b>		95°C (30 s)
<b>30 PCR cycles</b>	<b>Anneal</b>	55°C (30 s)
	<b>Extend</b>	72°C (30 s)
<b>Final Extension</b>		72°C (10 min)

## Statistical analysis

Statistical analysis was performed using GraphPad Prism 6 (GraphPad Software, San Diego, California). Significance between two datasets was assessed with a two-tailed unpaired Student t-test. Statistical comparison between more than two independent groups was performed with the Kruskal-Wallis test. P-values were calculated and statistical significance was considered when  $P < 0.05$ .

# Part III

## Results

# Chapter 8

## Diagnosis and prognosis

### 8.1 Human ADAMTS13 activity ELISA

The analysis of ADAMTS13 activity levels plays a pivotal role in TTP diagnosis, as ADAMTS13 activity below 10% is the only specific marker for TTP. However, the ADAMTS13 activity assays that are currently used are extremely expensive and requires substantial skill, especially the FRET assays. Therefore, an in-house VWF96 ADAMTS13 activity ELISA was developed, in collaboration with Dr. J. Crawley, for the use of citrated human plasma. This ELISA was based on the previously described VWF96 ADAMTS13 activity ELISA with recombinant ADAMTS13 (Schelpe, 2018). Citrate is used as an anticoagulant as it chelates divalent cations, making them unavailable to the clotting cascade. However, the anticoagulant also prevents these from binding in the M domain of ADAMTS13 and inhibits VWF proteolysis. The addition of the HBS buffer, the Bis-Tris buffer or the acetate buffer provides ADAMTS13 with the needed divalent cations and subsequently the proteolytic activity of ADAMTS13 can be tested. High ADAMTS13 activity, and thus high proteolysis of VWF96, results in the loss of the HSV tag at the C-terminal end of VWF96. Therefore, anti-HSV-HRP can no longer bind and lower OD values are expected. Accordingly, low ADAMTS13 activity does not result in proteolysis of VWF96 and the HSV-HRP antibody can recognize the C-terminal end of VWF96. Consequently, higher OD values are expected when ADAMTS13 activity is lower. The ADAMTS13 activity levels of undiluted NHP was set to 100%. The plate also contained four wells where no NHP was added, in accordance with 0% ADAMTS13 activity. The average OD value of these wells was used to calculate relative OD values. Not surprisingly, these average OD value were not significantly different for the three assay (n = 3 with P>0.05; data not shown).

Heparin (10 U/mL; LEO Pharma, Lier, Belgium) was added to the HBS and Bis-Tris buffer, as the dilution series of NHP in solely HBS or Bis-Tris buffer caused coagulation of the NHP sample (data not shown). Like citrate, heparin is an anticoagulant, however, its mechanism of action is antithrombin-dependent and does not work by chelating divalent cations. NHP dilutions series with solely acetate buffer did not result in coagulation of the NHP sample. However, the wells with the highest ADAMTS13 activity should result in lower relative OD values, as more VWF96 is proteolyzed, which was not the case (Figure 16 C). Hence, the acetate buffer is not appropriate for this ELISA set-up and was not used further.

The ELISA performed with Bis-Tris buffer (Figure 16 B) did not result in as efficient proteolysis of VWF96 as the ELISA performed with the HBS buffer (Figure 16 A). This is demonstrated in Figure 16 as higher relative OD values for higher activities are observed with the Bis-Tris buffer, although the average OD values used to calculate relative OD values were similar.

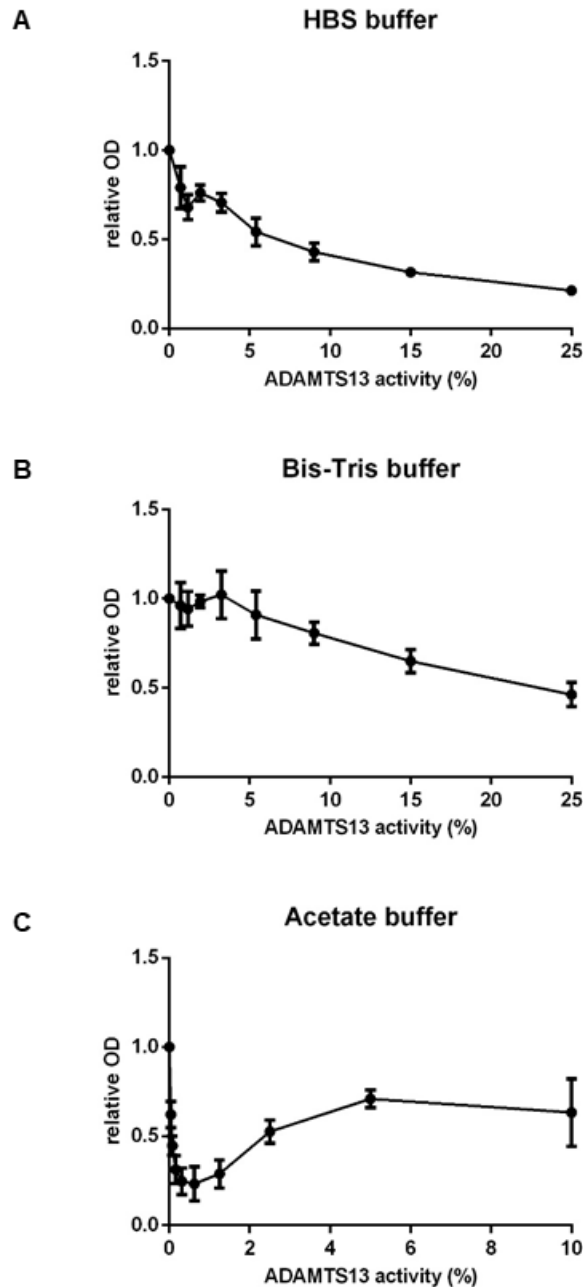


**Figure 16. Comparison of the ADAMTS13 activity ELISA data in different buffer systems.** NHP was serially diluted ( $n = 3$ ) with HBS buffer (A), Bis-Tris buffer (B) and acetate buffer (C) in a microtiter plate coated with anti-HisG and to which VWF96 was added. Unproteolyzed VWF96 was detected with anti-HSV antibody conjugated to HRP. The relative OD values of the ELISA performed with HBS ranged from  $0.21 \pm 0.02$  to 1. For the Bis-Tris buffer, the relative OD value ranged from  $0.46 \pm 0.07$  to 1.

## 8.2 Human anti-ADAMTS13 autoantibody ELISA

The measurement of anti-ADAMTS13 autoantibodies titers is crucial to distinguish between the two major forms of TTP. In the Laboratory for Thrombosis Research, the anti-ADAMTS13 autoantibody titers can be determined using the in-house anti-ADAMTS13 autoantibody ELISA. As a part of the characterisation process of this assay, a cut-off was established that can reliably discriminate between individuals with and without anti-ADAMTS13 autoantibodies. The cut-off was determined by measuring the anti-ADAMTS13 IgG autoantibody titer in a large cohort of HD plasma samples (n = 424). HD samples with an OD-value greater than 0.1 for the non-coated well were excluded (n = 20). The IgG autoantibody titer of the remaining HD samples (n = 404) were calculated and ranged from 0.41% to 22.07%, with a mean of 2.39% ± 1.90%. The cut-off was established at the 97.5<sup>th</sup> percentile (6.70%). The anti-ADAMTS13 IgG autoantibody titers of the 19 iTTP patient plasma samples were measured and ranged from 5.14% to 135.10%, with a mean of 43.24 ± 41.43%. The autoantibody titers of the iTTP patient plasma samples were used to conclusively show the validity of the cut-off value. All iTTP patients, except one (5.14%; shown in red), had an autoantibody titer above the cut-off value.

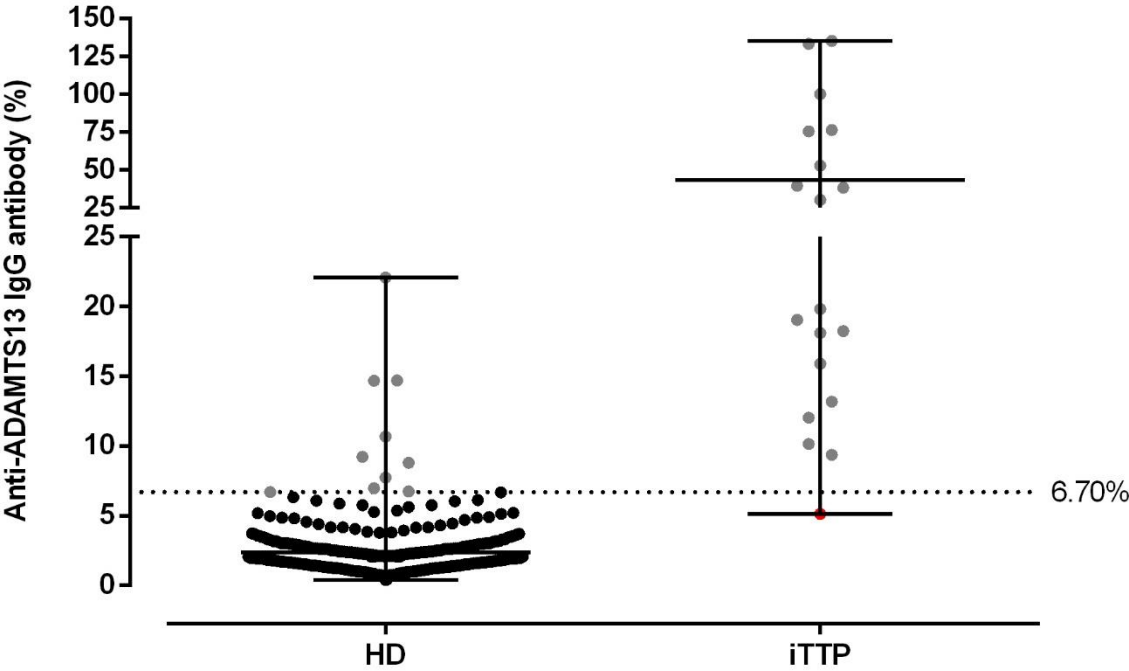


**Figure 17.** The cut-off value of the anti-ADAMTS13 autoantibody ELISA is 6.07%. The 97.5<sup>th</sup> percentile of the anti-ADAMTS13 IgG antibody titers of HDs (n = 404) was calculated at 6.70%. The antibody titers in the upper 2.5% are shown in grey. The lower 97.5% is shown in black. Antibody titers of iTTP patient samples are compared to the cut-off, one titer falls below the cut-off (5.14%, shown in red). Percentages are represented as mean with minimal and maximal range.

### 8.3 Human ADAMTS13 antigen binding ELISA

Recently, the significance of ADAMTS13 clearance as a causative factor of ADAMTS13 deficiency has become more clear as ADAMTS13 antigen (ADAMTS13:Ag) levels are often severely decreased in iTTP patients, even in the presence of inhibitory anti-ADAMTS13 autoantibodies (Alwan et al., 2017; Thomas et al., 2015). It was shown that a low ADAMTS13:Ag level at presentation is associated with higher mortality (Alwan et al., 2017; Feys et al., 2006; Rieger et al., 2006; Thomas et al., 2015; Yang et al., 2011) and a low ADAMTS13:Ag level at initial clinical response is associated with a higher risk of exacerbation or relapse (Yang et al., 2011). Nevertheless, ADAMTS13 antigen measurements are not routinely performed.

In the Laboratory for Thrombosis Research ADAMTS13:Ag levels can be measured using the in-house ADAMTS13 antigen ELISA. To characterise this assay the ADAMTS13:Ag levels of a large cohort of samples were measured. Initially, ADAMTS13:Ag levels of 424 HDs were determined. The reference range obtained for ADAMTS13:Ag in this group was 0.26-1.50 U/mL plasma with a mean of  $0.87 \pm 0.16$  U/mL. Next, the ADAMTS13 antigen levels of 19 iTTP patients were analysed. The amount of ADAMTS13:Ag ranged from 0-0.28 U/mL, with a mean of  $0.11 \pm 0.08$  U/mL. A significant difference ( $P < 0.0001$ ) between the ADAMTS13:Ag levels of HDs and iTTP patient plasma samples was found.

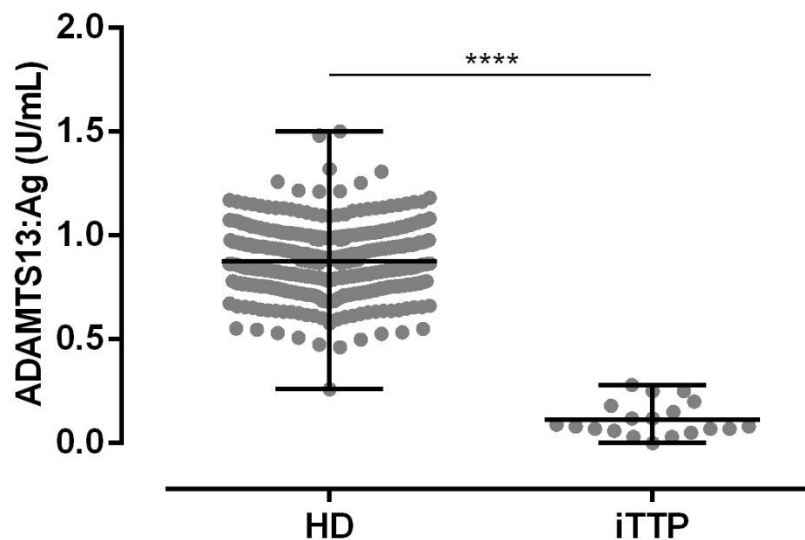


**Figure 18. ADAMTS13:Ag levels are significantly reduced in iTTP patient plasma samples.** The ADAMTS13:Ag levels 424 HDs and 19 iTTP patient plasma samples were compared. Data is represented as mean with minimal and maximal range with \*\*\*\* $P < 0.0001$ .

# Chapter 9

## Gene therapy

### 9.1 Construction of the pMA-CAG-mADAMTS13 plasmid

The pMA-CAG-TMab2\_LC#9 vector was linearized using two restriction enzymes, *AgeI* and *BstBI* and the mADAMTS13 DNA fragment was amplified from the pBS-II-SK-HCHRPi-mADAMTS13 vector. DNA gel electrophoresis of the digested pMA-CAG-Tmab2\_LC#9 vector resulted in a band size of approximately 4060 bp and the mADAMTS13 PCR product resulted in a band size of approximately 4890 bp, which confirmed that linearization and amplification worked. Then, the DNA fragments were excised from the gel for purification (Figure 19).

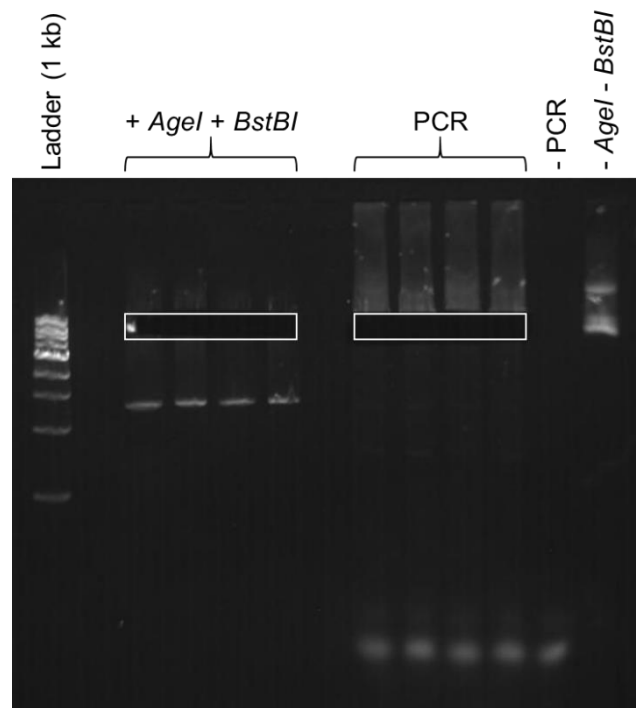


**Figure 19. Excision of the linearized vector and mADAMTS13 PCR product from a 1% agarose gel.** After verification of the pMA-CAG-Tmab2\_LC#9 vector digestion (+ *AgeI* + *BstBI*) and amplification of the mADAMTS13 DNA fragment from the pBS-II-SK-HCHRPi-mADAMTS13 vector (PCR), the appropriate bands were excised. Negative controls included a MQ control for the amplification (-PCR), as well as the digestion mixture, including the pMA-CAG-Tmab2\_LC#9 vector, without the restriction enzymes (- *AgeI* - *BstBI*). The 1 kb ladder was used as a reference.

Thereafter, the concentrations of the purified products were estimated at 200 ng/5  $\mu$ L for the linearized vector and 80 ng/5  $\mu$ L for the mADAMTS13 PCR product (Figure 21).

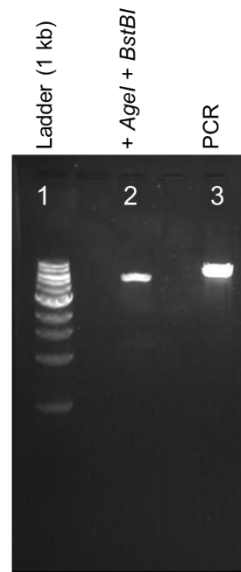


**Figure 20. Concentration estimation of the purified products.** 5  $\mu$ L of the purified linearized vector (+ *AgeI* + *BstBI*) and the purified mADAMTS13 PCR product (PCR) were run on a 1% agarose gel. Concentration were estimated using the 1 kb ladder as a reference.

The purified products were cloned using the In-Fusion® HD Cloning Kit resulting in the pMA-CAG-mADAMTS13 plasmid (Figure 21).

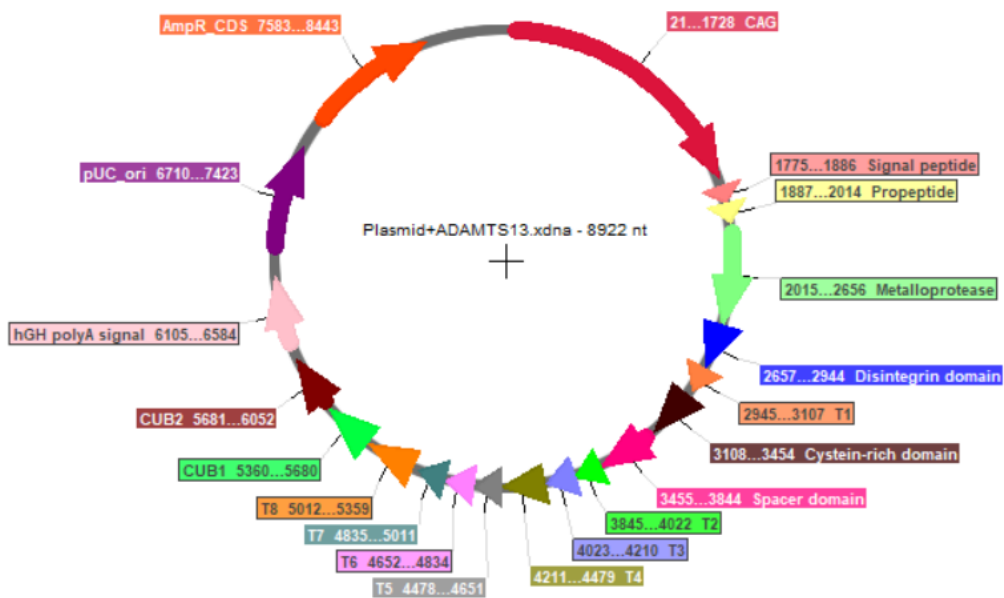


**Figure 21. Vector map of cloned pMA-CAG-mADAMTS13 plasmid.**

Chemically competent NovaBlue cells were transformed with the constructed plasmid and spread on ampicillin selective agar plates to screen for the presence of the plasmid. Then, the plasmid DNA of twelve individual and different colonies was isolated and purified. The presence of the *mADAMTS13* gene was verified using PCR (Figure 22).

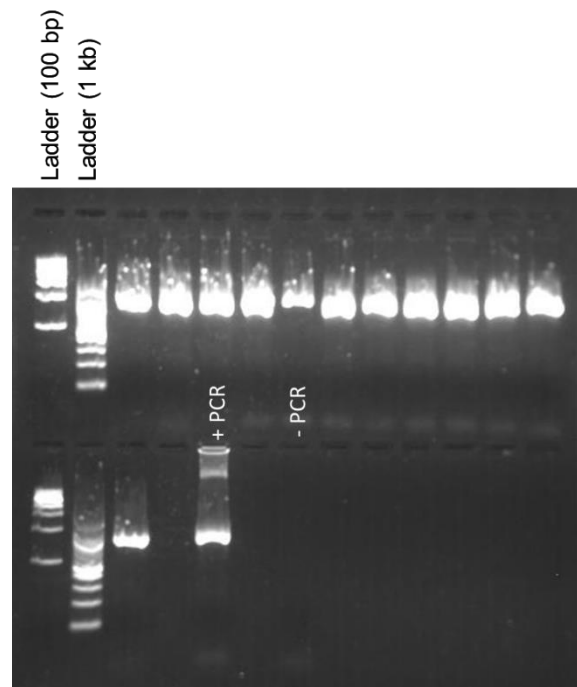


**Figure 22. Positive detection of *mADAMTS13* cDNA in the plasmid DNA of twelve colonies.** The constructed plasmid was amplified and plasmid DNA was isolated from twelve distinctive colonies. Next, the presence of the *mADAMTS13* gene was analysed using PCR and verified on a 1.5% agarose gel using the 100 bp and 1 kb ladder as a reference. The pBS-II-SK-HCHRPi-*mADAMTS13* vector was included as a positive control (+ PCR). A MQ control was used as a negative control (-PCR).

The plasmid DNA of all twelve colonies contained *mADAMTS13* cDNA. Three samples were chosen and sent to LGC Genomics (Berlin, Germany) to confirm the orientation of the *mADAMTS13* via sequencing. All three contained *mADAMTS13* in the correct orientation, and thus one plasmid was selected for full sequencing of the *mADAMTS13* gene. The *mADAMTS13* gene of the chosen plasmid did not contain any mutations and was used in subsequent *in vitro* testing.

## 9.2 *In vitro* testing of the pMA-CAG-mADAMTS13 plasmid

After the transfection of C2C12 cells, a mouse myoblast cell line, with the selected plasmid, the transgene expression was evaluated via the mADAMTS13 antigen ELISA as previously described (De Cock et al., 2015; Deforche et al., 2016). As illustrated in Figure 23, the relative OD values, representing mADAMTS13 expression levels, were significantly higher ( $P < 0.0001$ ) in the medium of C2C12 cells transfected with pMA-CAG-mADAMTS13 ( $0.66 \pm 0.25$ ) in comparison to the relative OD values of the negative control ( $0.074 \pm 0.02$ ).

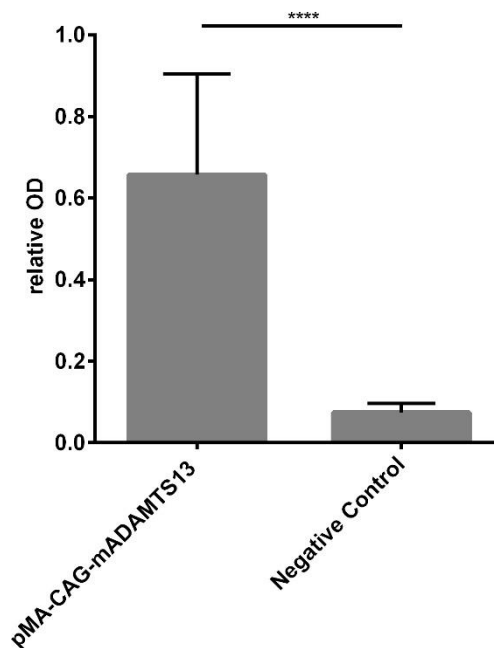


**Figure 23. Relative OD values are significantly increased in expression medium of C2C12 cells transfected with the constructed plasmid.** OD values of C2C12 cells transfected with the constructed pMA-CAG-mADAMTS13 plasmid and non-transfected cells were determined via the mADAMTS13 antigen ELISA. Data are represented as relative OD values (mean + SD,  $n = 12$  with \*\*\*\* $P < 0.0001$ ) with the OD value of NMP (diluted 1/80) set to 1 as a reference.

## 9.3 Preparation of the pMA-CAG-mADAMTS13 plasmid

The pMA-CAG-mADAMTS13 plasmid will be used for *in vivo* experiments in the near future. The plasmid will be introduced into the muscle cells of *Adamts13* knockout mice via intramuscular electrotransfer. Therefore, the pMA-CAG-mADAMTS13 plasmid was produced in large quantities and purified. The resulting concentration was approximately 3.53 mg/mL buffer (provided with the EndoFree Plasmid Mega Kit).

## 9.4 Creation of immunodeficient *Adamts13* knockout mice

*Adamts13*<sup>-/-</sup> mice (*ADAMTS13*<sup>mut/mut</sup>*RAG1*<sup>WT/WT</sup>) were crossed with *RAG1*-deficient mice (*ADAMTS13*<sup>WT/WT</sup>*RAG1*<sup>mut/mut</sup>) to generate double knockout mice (*ADAMTS13*<sup>mut/mut</sup>*RAG1*<sup>mut/mut</sup>). The *RAG1*-deficient mice are homozygous for the *Rag1*<sup>tm1Mom</sup> mutation. Using ear tissue, the progeny was genotyped via PCR and PCR products were verified on a 1.8% agarose gel. Eventually, two female and two male double knockout mice were generated that will be used for further breeding (data not shown).

In Figure 24, “Mouse 1”, “Mouse 2” and “Mouse 3” represent the progeny of the crossings between *ADAMTS13*<sup>mut/mut</sup>*RAG1*<sup>WT/WT</sup> and *ADAMTS13*<sup>WT/WT</sup>*RAG1*<sup>mut/mut</sup> mice or subsequent crossing with the obtained offspring.

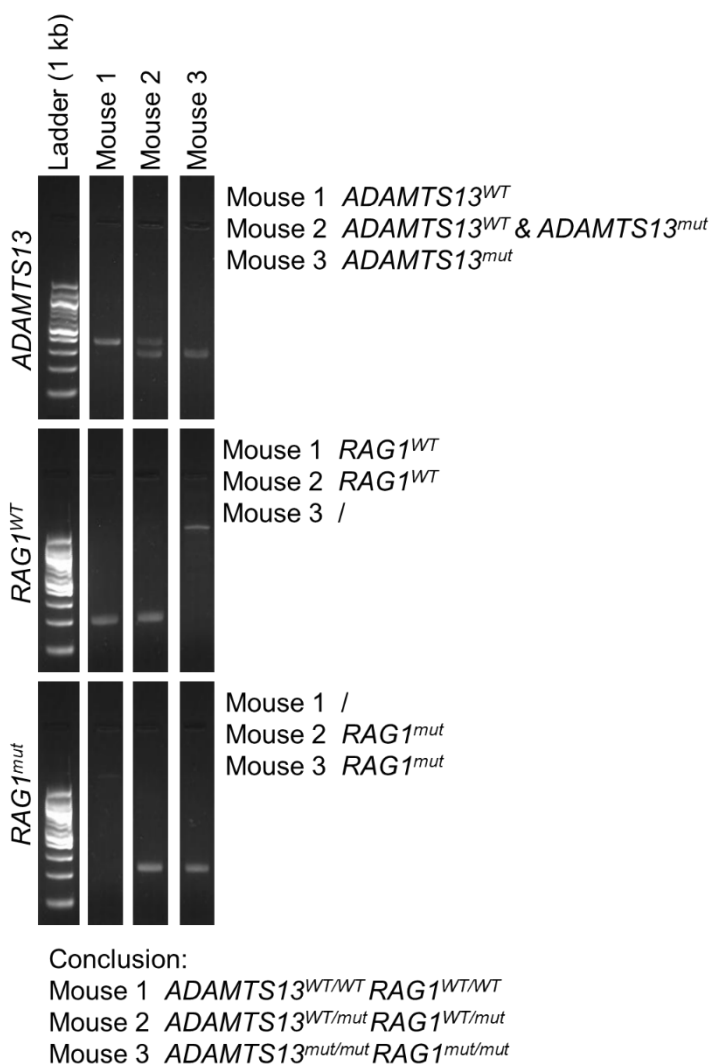


**Figure 24. PCR-based genotyping of representative progeny of performed crossings.** Results for mice representing all three genotypes (WT/WT; WT/mut; mut/mut) of both *ADAMTS13* and *RAG1*. The band produced by the primers for the *ADAMTS13*<sup>WT</sup> allele is approximately 400 bp and the band produced by the primers for the *ADAMTS13*<sup>mut</sup> allele is approximately 300 bp. The band produced by the primer sets for the *RAG1*<sup>WT</sup> and *RAG1*<sup>mut</sup> alleles is approximately 200 bp, hence, the PCR assays are performed separately.

Part IV

Discussion

# Chapter 10

## Diagnosis and prognosis

### 10.1 Human ADAMTS13 activity ELISA

The diagnosis of TTP remains a hurdle as the clinical signs and symptoms vary extremely between patients and show overlap with other TMAs. Consequently, the measurement of ADAMTS13 activity plays a pivotal role in the diagnostic process of a TTP patient, as ADAMTS13 activity below 10% results in the differential diagnosis of TTP. Currently, ADAMTS13 activity levels are determined using FRET assays, such as the FRET-S-VWF73 (Kokame et al., 2005) and the FRET-S-rVWF71 (Muia et al., 2013), or the TECHNOZYM ADAMTS-13 Activity ELISA (Technoclone, Vienna, Austria). The FRET-assays cost approximately 10\$/data point (US20130023004A1, 2013) and require special equipment to measure fluorescence, as well as substantial technical skill (Sadler, 2015). Moreover, the fluorogenic substrates used in these assays are patented (US8663912B2, 2014) and the production of the substrates is labour-intensive. Although ELISA assays are generally less expensive than FRET-assays, the TECHNOZYM ADAMTS-13 Activity ELISA is also extremely expensive and the principle behind this assay is also patented (EP1852442B1, 2012).

Therefore, some adaptations were made to the VWF96 ADAMTS13 activity ELISA (Schelpe, 2018) to be able to use citrated human plasma as a source of ADAMTS13, instead of recombinant ADAMTS13. The HBS activity buffer (De Cock et al., 2015) with heparin (10 U/mL) showed the most promising results. However, further optimisation of this ELISA is needed, as the sensitivity was very low, especially considering that TTP patients have an ADAMTS13 activity below 10%. The HBS buffer contains  $\text{CaCl}_2$  and  $\text{ZnCl}_2$  to counteract the reduction of free divalent ions due to chelation by citrate, as this chelation inhibits ADAMTS13 activity. Accordingly, heparin had to be added to the buffer to prevent coagulation of the NHP sample. Heparin accelerates the inhibiting effect that antithrombin has on factor IIa and factor Xa, as well as some other enzymes of the coagulation cascade.

### 10.2 Human anti-ADAMTS13 autoantibody ELISA

To distinguish between the two main types of TTP, cTTP and iTTP, the presence of anti-ADAMTS13 autoantibodies is analysed (Figure 8). A patient with ADAMTS13 activity <10% during the acute TTP episode and detectable anti-ADAMTS13 autoantibodies is diagnosed with iTTP. Patients are diagnosed with cTTP when their ADAMTS13 activity levels are always <10%, no anti-ADAMTS13 autoantibodies are detected and the presence of mutations in the *ADAMTS13* gene is confirmed (Joly et al., 2017a; Knöbl, 2018). Thus, the measurement of

anti-ADAMTS13 autoantibodies is an important part of the diagnostic procedure, especially as genomic analysis of the *ADAMTS13* gene is often only performed if autoantibody detection was negative (Joly et al., 2017a).

In the Laboratory for Thrombosis Research, the anti-ADAMTS13 autoantibody titers are determined using the in-house anti-ADAMTS13 autoantibody ELISA. Here, the analysis of 424 HDs samples, of which 20 were excluded due to a high background signal in the non-coated well, were used to calculate the cut-off value of this assay (6.70%) relative to a high titer plasma sample. This value is crucial as it discriminates between individuals with and without anti-ADAMTS13 autoantibodies, and can be used for the diagnosis of iTTP, and consequently cTTP. All iTTP patients plasma samples, except one, had a detectable autoantibody titer above the cut-off value.

### 10.3 Human ADAMTS13 antigen binding ELISA

The mortality rate of TTP remains 10-20% and after the initial TTP episode one third of all patients relapse one or multiple times. Unfortunately, the knowledge about factors that can assess the severity of an acute TTP episode and predict treatment outcome, as well as disease prognosis, is limited. However, several recent studies have demonstrated that the ADAMTS13 antigen level is an extremely valuable biomarker of poor prognosis. A better understanding of ADAMTS13 antigen levels, in both healthy donors and patients, is of great value. Consequently, the characterisation and validation of the in-house ADAMTS13 antigen binding ELISA used in the Laboratory for Thrombosis Research is a next important step. Therefore, the ADAMTS13 antigen levels of a large cohort of samples, including 424 healthy donor and 19 iTTP patient plasma samples, were measured using the in-house ELISA. The reference interval of ADAMTS13 antigen levels in the plasma spanned 0.26-1.50 U/mL with a mean of  $0.87 \pm 0.16$  U/mL. Accordingly as to what was previously found, the ADAMTS13 antigen levels of the 19 iTTP patients were significantly lower, ranging from 0-0.28 U/mL. Based on these results, two HD samples, one sample with a relatively high ADAMTS13 antigen and one with a relatively low ADAMTS13 antigen, and two iTTP patient samples, again one with a relatively high and one with a relatively low ADAMTS13 antigen were selected for validation of the assay.

# Chapter 11

## Gene therapy

In patients with cTTP, plasma infusions are used to provide the missing functional ADAMTS13 when they experience an acute TTP episode. However, some patients need lifelong prophylactic treatment to prevent chronic relapsing. Considering the severity of TTP, as every acute TTP episode is life-threatening, and the severe limitations of plasma infusion, gene therapy might provide an alternative. Especially because an ADAMTS13 activity of 10% should be sufficient to protect the patients against disease recurrences (Trionfini et al., 2009) and because the underlying genetic defect is monogenic. Several gene therapy approaches for cTTP have been tested in preclinical mouse models and provide proof of concept. However, gene delivery methods that are clinically relevant for humans are needed, such as the intramuscular electotransfer of plasmid DNA.

The pMA-CAG-mADAMTS13 plasmid was cloned, which contains the murine *ADAMTS13* gene under the control of the CAG promotor, a general promotor with high activity in the muscles (Aihara & Miyazaki, 1998). Gene expression was assessed *in vitro* in the murine myoblast C2C12 cell line. The C2C12 cells transfected with the pMA-CAG-mADAMTS13 plasmid expressed and secreted ADAMTS13. This provides a rationale to further analyse ADAMTS13 expression from the pMA-CAG-mADAMTS13 plasmid *in vivo*. The *in vivo* experiments require both immune-competent and immune-compromised *Adamts13*<sup>-/-</sup> mice to analyse *in vivo* expression and ADA response as anti-drug antibodies could prevent long-term expression of ADAMTS13, as well as the possibility to re-dose the patient with the plasmid if necessary. Thus, *Adamts13*<sup>-/-</sup>*Rag1*<sup>tm1Mom/tm1Mom</sup> mice were bred by crossing *Adamts13*<sup>-/-</sup> and *Rag1*<sup>tm1Mom/tm1Mom</sup> mice.

# References

- Aihara, H., & Miyazaki, J. (1998). Gene transfer into muscle by electroporation in vivo. *Nat. Biotechnol.*, *16*(9), 867–870.
- Alwan, F., Vendramin, C., Vanhoorelbeke, K., et al. (2017). Presenting ADAMTS13 antibody and antigen levels predict prognosis in immune-mediated thrombotic thrombocytopenic purpura. *Blood*, *130*(4), 466–471.
- Amorosi, E. L., & Ultmann, J. E. (1966). Thrombotic thrombocytopenic purpura: report of 16 cases and review of the literature. *Medicine*, *45*(2), 139–160.
- Anderson, P. J., Kokame, K., & Sadler, J. E. (2006). Zinc and calcium ions cooperatively modulate ADAMTS13 activity. *J. Biol. Chem.*, *281*(2), 850–857.
- André, F., & Mir, L. M. (2004). DNA electrotransfer: its principles and an updated review of its therapeutic applications. *Gene Ther.*, *11*(Suppl 1), S33–S42.
- Blombäck, M., Eikenboom, J., Lane, D., Denis, C., & Lillicrap, D. (2012). von Willebrand disease biology. *Haemophilia*, *18*(Suppl 4), 141–147.
- Blombery, P., & Scully, M. (2014). Management of thrombotic thrombocytopenic purpura : current perspectives. *J. Blood Med.*, *5*, 15–23.
- Boulpaep, E. L. (2017). Blood. In Boron, W. F., & Boulpaep, E. L. (Eds.), *Medical Physiology* (pp. 429–446). Philadelphia, PA: Elsevier.
- Cataland, S. R., Yang, S., Witkoff, L., Kraut, E. H., Lin, S., George, J. N., & Wu, H. M. (2009). Demographic and ADAMTS13 biomarker data as predictors of early recurrences of idiopathic thrombotic thrombocytopenic purpura. *Eur. J. Haematol.*, *83*(6), 559–564.
- Chapin, J. C., & Hajjar, K. A. (2015). Fibrinolysis and the control of blood coagulation. *Blood Reviews*, *29*(1), 17–24.
- Coppo, P., Cuker, A., & George, J. N. (2019). Thrombotic thrombocytopenic purpura : Toward targeted therapy and precision medicine. *Res. Pract. Thromb. Haemost.*, *3*(1), 26–37.
- Crawley, J. T. B., de Groot, R., Xiang, Y., Luken, B. M., & Lane, D. A. (2011). Unraveling the scissile bond: how ADAMTS13 recognizes and cleaves von Willebrand factor. *Blood*, *118*(12), 3212–3221.
- De Cock, E., Hermans, C., De Raeymaecker, J., et al. (2015). The novel ADAMTS13-p.D187H mutation impairs ADAMTS13 activity and secretion and contributes to thrombotic thrombocytopenic purpura in mice. *J. Thromb. Haemost.*, *13*(2), 283–292.
- Deforche, L., Tersteeg, C., Roose, E., et al. (2016). Generation of anti-murine ADAMTS13 antibodies and their application in a mouse model for acquired thrombotic thrombocytopenic purpura. *PLoS ONE*, *11*(8), 1-15.
- de Groot, R., Lane, D. A., & Crawley, J. T. B. (2010). The ADAMTS13 metalloprotease domain: roles of subsites in enzyme activity and specificity. *Blood*, *116*(16), 3064–3072.
- de Groot, R., Lane, D. A., & Crawley, J. T. B. (2015). The role of the ADAMTS13 cysteine-rich domain in VWF binding and proteolysis. *Blood*, *125*(12), 1968–1975.

- de Laat, B., van Berkel, M., Urbanus, R. T., Siregar, B., de Groot, P. G., Gebbink, M. F., & Maas, C. (2011). Immune responses against domain I of  $\beta$ 2-glycoprotein I are driven by conformational changes: Domain I of  $\beta$ 2-glycoprotein I harbors a cryptic immunogenic epitope. *Arthritis Rheum.*, 63(12), 3960–3968.
- Ercig, B., Wichapong, K., Reutelingsperger, C. P. M., Vanhoorelbeke, K., Voorberg, J., & Nicolaes, G. A. F. (2018). Insights into 3D Structure of ADAMTS13: A Stepping Stone towards Novel Therapeutic Treatment of Thrombotic Thrombocytopenic Purpura. *Thromb Haemost.*, 118(1), 28–41.
- Feng, Y., Li, X., Xiao, J., Li, W., Liu, J., Zeng, X., Chen, X., & Chen, S. (2016). ADAMTS13: more than a regulator of thrombosis. *International Journal of Hematology*, 104(5), 534–539.
- Ferrari, S., Palavra, K., Gruber, B., et al. (2014). Persistence of circulating ADAMTS13-specific immune complexes in patients with acquired thrombotic thrombocytopenic purpura. *Haematologica*, 99(4), 779–787.
- Feys, H. B., Liu, F., Dong, N., et al. (2006). ADAMTS-13 plasma level determination uncovers antigen absence in acquired thrombotic thrombocytopenic purpura and ethnic differences. *J. Thromb. Haemost.*, 4(5), 955–962.
- Finley, A., & Greenberg, C. (2013). Heparin sensitivity and resistance: management during cardiopulmonary bypass. *Anesth. Analg.*, 116(6), 1210–1222.
- Furlan, M., Robles, R., & Lämmle, B. (1996). Partial purification and characterization of a protease from human plasma cleaving von Willebrand factor to fragments produced by in vivo proteolysis. *Blood*, 87(10), 4223–4234.
- George, J. N. (2010). How I treat patients with thrombotic thrombocytopenic purpura: 2010. *Blood*, 116(20), 4060–4069.
- Grall, M., Azoulay, E., Galicier, L., et al. (2017). Thrombotic thrombocytopenic purpura misdiagnosed as autoimmune cytopenia: Causes of diagnostic errors and consequence on outcome. Experience of the French thrombotic microangiopathies reference centre. *Am. J. Hematol.*, 92(4), 381–387.
- Grillberger, R., Casina, V. C., Turecek, P. L., Zheng, X. L., Rottensteiner, H., & Scheifflinger, F. (2014). Anti-ADAMTS13 IgG autoantibodies present in healthy individuals share linear epitopes with those in patients with thrombotic thrombocytopenic purpura. *Haematologica*, 99(4), e58–e60.
- Hollevoet, K., De Smidt, E., Geukens, N., & Declerck, P. (2018). Prolonged in vivo expression and anti-tumor response of DNA- based anti-HER2 antibodies. *Oncotarget*, 9(17), 13623–13636.
- Hollevoet, K., & Declerck, P. J. (2017). State of play and clinical prospects of antibody gene transfer. *Journal of Translational Medicine*, 15(131).
- James, P. D., & Lillicrap, D. (2013). The molecular characterization of von Willebrand disease: good in parts. *Br. J. Haematol.*, 161(2), 166–176.
- Jin, S., Xiao, J., Bao, J., Zhou, S., Wright, J. F., & Zheng, X. L. (2013). AAV-mediated expression of an ADAMTS13 variant prevents shigatoxin-induced thrombotic thrombocytopenic purpura. *Blood*, 121(19), 3825–3829.
- Joly, B. S., Coppo, P., & Veyradier, A. (2017). Thrombotic thrombocytopenic purpura. *Blood*, 129(21), 2836–2847. (a)

- Joly, B. S., Vanhoorelbeke, K., & Veyradier, A. (2017). Understanding therapeutic targets in thrombotic thrombocytopenic purpura. *Intensive Care Med.*, 43(9), 1398–1400. (b)
- Kato, S., Hiura, H., Fujimura, Y., & Matsumoto, M. (2012). *European Patent No. EP1852442B1*. Retrieved from <https://patents.google.com/patent/EP1852442B1/en>.
- Kato, S., Matsumoto, M., Matsuyama, T., Isonishi, A., Hiura, H., & Fujimura, Y. (2006). Novel monoclonal antibody-based enzyme immunoassay for determining plasma levels of ADAMTS13 activity. *Transfusion*. 46(8), 1444–1452.
- Katsumi, A., Tuley, E. A., Bodó, I., & Sadler, J. E. (2000). Localization of Disulfide Bonds in the Cystine Knot Domain of Human von Willebrand Factor. *J. Biol. Chem.*, 275(33), 25585–25594.
- Knöbl, P. (2018). Thrombotic thrombocytopenic purpura. *Memo*, 11(3), 220–226.
- Kokame, K., Nobe, Y., Kokubo, Y., Okayama, A., & Miyata, T. (2005). FRETTS-VWF73, a first fluorogenic substrate for ADAMTS13 assay. *Br. J. Haematol.*, 129(1), 93–100.
- Koyama, N., Matsumoto, M., Tamaki, S., Yoshikawa, M., Fujimura, Y., & Kimura, H. (2012). Reduced larger von Willebrand factor multimers at dawn in OSA plasmas reflect severity of apnoeic episodes. *Eur. Respir. J.*, 40(3), 657–664.
- Kreimann, M., Brandt, S., Krauel, K., Block, S., Helm, C. A., Weitschies, W., Greinacher, A., & Delcea, M. (2014). Binding of anti-platelet factor 4/heparin antibodies depends on the thermodynamics of conformational changes in platelet factor 4. *Blood*, 124(15), 2442–2449.
- Kremer Hovinga, J. A., Vesely, S. K., Terrell, D. R., Lämmle, B., & George, J. N. (2010). Survival and relapse in patients with thrombotic thrombocytopenic purpura. *Blood*, 115(8), 1500–1511.
- Kremer Hovinga, J. A., & Voorberg, J. (2012). Improving on nature: redesigning ADAMTS13. *Blood*, 119(16), 3654–3655.
- Kremer Hovinga, J. A., & Lämmle, B. (2012). Role of ADAMTS13 in the pathogenesis, diagnosis, and treatment of thrombotic thrombocytopenic purpura. *Hematol. Am. Soc. Hematol. Educ. Progr. 2012*, 1, 610–616.
- Kremer Hovinga, J. A., Coppo, P., Lämmle, B., Moake, J. L., Miyata, T., & Vanhoorelbeke, K. (2017). Thrombotic thrombocytopenic purpura. *Nat. Rev. - Dis. Prim.*, 3, 1-17.
- Laje, P., Shang, D., Cao, W., et al. (2009). Correction of murine ADAMTS13 deficiency by hematopoietic progenitor cell-mediated gene therapy. *Blood*, 113(10), 2172–2180.
- Lam, J. K., Chion, C. K. N. K., Zanardelli, S., Lane, D. A., & Crawley, J. T. B. (2007). Further characterization of ADAMTS-13 inactivation by thrombin. *J. Thromb. Haemost.*, 5(5), 1010–1018.
- Lämmle, B., Kremer Hovinga, J. A., & Alberio, L. (2005). Thrombotic thrombocytopenic purpura. *J. Thromb. Haemost.*, 3(8), 1663–1675.
- Lenting, P. J., Christophe, O. D., & Denis, C. V. (2015). von Willebrand factor biosynthesis, secretion, and clearance: connecting the far ends. *Blood*, 125(13), 2019–2028.
- Levy, G. G., Nichols, W. C., Lian, E. C., et al. (2001). Mutations in a member of the ADAMTS gene family cause thrombotic thrombocytopenic purpura. *Nature*, 413(6855), 488–494.
- Lillicrap, D. (2013). von Willebrand disease: advances in pathogenetic understanding, diagnosis, and therapy. *Blood*, 122(23), 3735–3740.

- Liu-Chen, S., Connolly, B., Cheng, L., Subramanian, R. R., & Han, Z. (2018). mRNA treatment produces sustained expression of enzymatically active human ADAMTS13 in mice. *Sci. Rep.*, *8*, 7859.
- Lopes da Silva, M., & Cutler, D. F. (2016). von Willebrand factor multimerization and the polarity of secretory pathways in endothelial cells. *Blood*, *128*(2), 277–285.
- Lotta, L. A., Garagiola, I., Palla, R., Cairo, A., & Peyvandi, F. (2010). ADAMTS13 mutations and polymorphisms in congenital thrombotic thrombocytopenic purpura. *Hum. Mutat.*, *31*(1), 11–19.
- Luo, G., Ni, B., Yang, X., & Wu, Y. (2012). von Willebrand Factor: More Than a Regulator of Hemostasis and Thrombosis. *Acta Haematol.*, *128*(3), 158–169.
- Mancini, I., Ferrari, B., Valsecchi, C., Pontiggia, S., Fornili, M., Biganzoli, E., & Peyvandi, F. (2017). ADAMTS13-specific circulating immune complexes as potential predictors of relapse in patients with acquired thrombotic thrombocytopenic purpura. *Eur. J. Intern. Med.*, *39*, 79–83.
- Martino, S., Jamme, M., Deligny, C., et al. (2016). Thrombotic Thrombocytopenic Purpura in Black People: Impact of Ethnicity on Survival and Genetic Risk Factors. *PLOS ONE*, *11*(7), 3-12.
- Moake, J. L., Rudy, C. K., Troll, J. H., Weinstein, M. J., Colannino, N. M., Azocar, J., Seder, R. H., Suchen L. H., & Deykin, D. (1982). Unusually large plasma factor VIII: von Willebrand factor multimers in chronic relapsing thrombotic thrombocytopenic purpura. *N. Engl. J. Med.*, *307*(23), 1432–1435.
- Mombaerts, P., Iacomini, J., Johnson, R. S., Herrup, K., Tonegawa, S., & Papaioannou, V. E. (1992). RAG-1-Deficient Mice Have No Mature B and T Lymphocytes. *Cell*, *68*, 869–877.
- Monroe, D. M., & Hoffman, M. (2006). What Does It Take to Make the Perfect Clot? *Arterioscler. Thromb. Vasc. Biol.*, *26*(1), 41–48.
- Motto, D. G., Chauhan, A. K., Zhu, G., et al. (2005). Shigatoxin triggers thrombotic thrombocytopenic purpura in genetically susceptible ADAMTS13-deficient mice. *J. Clin. Invest.*, *115*(10), 2752–2761.
- Muia, J., Gao, W., Haberichter, S. L., Dolatshahi, L., Zhu, J., Westfield, L. A., Covill, S. C., & Sadler, J. E. (2013). An optimized fluorogenic ADAMTS13 assay with increased sensitivity for the investigation of patients with thrombotic thrombocytopenic purpura. *J. Thromb. Haemost.*, *11*(8), 1511–1518.
- Muia, Joshua, Zhu, J., Gupta, G., et al. (2014). Allosteric activation of ADAMTS13 by von Willebrand factor. *Proc. Natl. Acad. Sci.*, *111*(52), 18584–18589.
- Müller, J. P., Mielke, S., Löf, A., et al. (2016). Force sensing by the vascular protein von Willebrand factor is tuned by a strong intermonomer interaction. *Proc. Natl. Acad. Sci.*, *113*(5), 1208–1213.
- Murphy, K., & Weaver, C. (2017). *Janeway's immunobiology* (9<sup>th</sup> ed.). New York, NY: Garland Science.
- Niiya, M., Endo, M., Shang, D., et al. (2009). Correction of ADAMTS13 Deficiency by In Utero Gene Transfer of Lentiviral Vector encoding ADAMTS13 Genes. *Mol. Ther.*, *17*(1), 34–41.

- Peyvandi, F., Scully, M., Kremer Hovinga, J. A., et al. (2016). Caplacizumab for Acquired Thrombotic Thrombocytopenic Purpura. *N. Engl. J. Med.*, 374(6), 511–522.
- Plautz, W. E., Raval, J. S., Dyer, M. R., Rollins-Raval, M. A., Zuckerbraun, B. S., & Neal, M. D. (2018). ADAMTS13: origins, applications, and prospects. *Transfusion*, 58(10), 2453–2462.
- Rauch, A., Wohner, N., Christophe, O. D., Denis, C. V., Susen, S., & Lenting, P. J. (2013). On the versatility of von Willebrand Factor. *Mediterr J Hematol Infect Dis.*, 5(1), e2013046.
- Raval, J. S., Padmanabhan, A., Kremer Hovinga, J. A., & Kiss, J. E. (2015). Development of a clinically significant ADAMTS13 inhibitor in a patient with hereditary thrombotic thrombocytopenic purpura. *Am. J. Hematol.*, 90(1), E22.
- Reininger, A. J. (2008). Function of von Willebrand factor in haemostasis and thrombosis. *Haemophilia*, 14(Suppl 5), 11–26.
- Rieger, M., Ferrari, S., Kremer Hovinga, J. A., et al. (2006). Relation between ADAMTS13 activity and ADAMTS13 antigen levels in healthy donors and patients with thrombotic microangiopathies (TMA). *Thromb Haemost.*, 95(2), 212–220.
- Roose, E., Schelpe, A., Joly, B. S., et al. (2018). An open conformation of ADAMTS-13 is a hallmark of acute acquired thrombotic thrombocytopenic purpura. *J. Thromb. Haemost.*, 16(2), 378–388. (a)
- Roose, E., Vidarsson, G., Kangro, K., et al. (2018). Anti-ADAMTS13 Autoantibodies against Cryptic Epitopes in Immune-Mediated Thrombotic Thrombocytopenic Purpura. *Thromb Haemost.*, 118(10), 1729–1742. (b)
- Ruggeri, Z. M. (2002). Platelets in atherothrombosis. *Mayo Clinic Proceedings. Mayo Clinic*, 8(11), 1227–1234.
- Sadler, J. E. (2002). A new name in thrombosis, ADAMTS13. *Proc. Natl. Acad. Sci.*, 99(18), 11552–11554.
- Sadler, J. E. (2015). What's new in the diagnosis and pathophysiology of thrombotic thrombocytopenic purpura. *Hematol. Am. Soc. Hematol. Educ. Progr.* 2015, 1, 631–636.
- Sadler, J. E. (2017). Pathophysiology of thrombotic thrombocytopenic purpura. *Blood*, 130(10), 1181–1188.
- Sadler, J. E., Muia, J., & Weiqiang, G. (2013). United States Patent No. US20130023004A1. Retrieved from <https://patents.google.com/patent/US20130023004A1/en>.
- Sadler, J. E., Muia, J., & Weiqiang, G. (2014). United States Patent No. US8663912B2. Retrieved from <https://patents.google.com/patent/US8663912B2/en>.
- Sanders, Y. V., Groeneveld, D., Meijer, K., et al. (2015). von Willebrand factor propeptide and the phenotypic classification of von Willebrand disease. *Blood*, 125(19), 3006–3013.
- Schelpe, A., Orlando, C., Ercig, B., et al. (2018). Child-onset thrombotic thrombocytopenic purpura caused by p.R498C and p.G259PfsX133 mutations in ADAMTS13. *Eur. J. Haematol.*, 101(2), 191–199.
- Schelpe, A. (2018). *Anti-ADAMTS13 antibodies: Insights into ADAMTS13 biology and thrombotic thrombocytopenic purpura pathophysiology using novel anti-ADAMTS13 antibodies* (Doctoral dissertation). Leuven, Belgium: KU Leuven, Faculty of Science.

- Schiviz, A., Wuersch, K., Piskernik, C., Dietrich, B., Hoellriegl, W., Rottensteiner, H., Scheiflinger, F., Schwarz, H.P., & Muchitsch, E. M. (2012). A new mouse model mimicking thrombotic thrombocytopenic purpura: correction of symptoms by recombinant human ADAMTS13. *Blood*, *119*(25), 6128–6135.
- South, K., Luken, B. M., Crawley, J. T. B., Phillips, R., Thomas, M., Collins, R. F., Deforche, L., Vanhoorelbeke, K., & Lane, D. A. (2014). Conformational activation of ADAMTS13. *Proc. Natl. Acad. Sci.*, *111*(52), 18578–18583.
- South, K., Freitas, M. O., & Lane, D. A. (2017). A model for the conformational activation of the structurally quiescent metalloprotease ADAMTS13 by von willebrand factor. *J. Biol. Chem.*, *292*(14), 5760–5769.
- Stockschlaeder, M., Schneppenheim, R., & Budde, U. (2014). Update on von Willebrand factor multimers: Focus on high-molecular-weight multimers and their role in hemostasis. *Blood Coagul. Fibrinolysis*, *25*(3), 206–216.
- Tersteeg, C., Schiviz, A., De Meyer, S. F., Plaimauer, B., Scheiflinger, F., Rottensteiner, H., & Vanhoorelbeke, K. (2015). Potential for Recombinant ADAMTS13 as an Effective Therapy for Acquired Thrombotic Thrombocytopenic Purpura. *Arterioscler. Thromb. Vasc. Biol.*, *35*(11), 2336–2342.
- Thomas, M. R., de Groot, R., Scully, M. A., & Crawley, J. T. B. (2015). Pathogenicity of Anti-ADAMTS13 Autoantibodies in Acquired Thrombotic Thrombocytopenic Purpura. *EBioMedicine*, *2*(8), 942–952.
- Trionfini, P., Tomasoni, S., Galbusera, M., Motto, D., Longaretti, L., Corna, D., Remuzzi, G., & Benigni, A. (2009). Adenoviral-mediated gene transfer restores plasma ADAMTS13 antigen and activity in ADAMTS13 knockout mice. *Gene Ther.*, *16*(11), 1373–1379.
- Truett, G. E., Heeger, P., Mynatt, R. L., Truett, A. A., Walker, J. A., & Warman, M. L. (2000). Preparation of PCR-Quality Mouse Genomic DNA with Hot Sodium Hydroxide and Tris (HotSHOT). *BioTechniques*, *29*(1), 52–54.
- Tsai, H. (1996). Physiologic cleavage of von Willebrand factor by a plasma protease is dependent on its conformation and requires calcium ion. *Blood*, *87*(10), 4235–4244.
- Tsai, H. (2012). von Willebrand Factor, Shear Stress, and ADAMTS13 in Hemostasis and Thrombosis. *ASAIO J.*, *58*(2), 163–169.
- Underwood, M., Peyvandi, F., Garagiola, I., Machin, S., & Mackie, I. (2016). Degradation of two novel congenital TTP ADAMTS13 mutants by the cell proteasome prevents ADAMTS13 secretion. *Thrombosis Research*, *147*, 16–23.
- Vanhoorelbeke, K., Cauwenberghs, N., Vandecasteele, G., Vauterin, S., & Deckmyn, H. (2002). A Reliable von Willebrand Factor: Ristocetin Cofactor Enzyme-Linked Immunosorbent Assay to Differentiate between Type 1 and Type 2 von Willebrand Disease. *Seminars in Thrombosis and Hemostasis*, *28*(2), 161–166.
- Vanhoorelbeke, K., & De Meyer, S. F. (2013). Animal models for thrombotic thrombocytopenic purpura. *J Thromb Haemost*, *11*(Suppl 1), 2–10.
- Verhenne, S., Vandeputte, N., Pareyn, I., Izsvák, Z., Rottensteiner, H., Deckmyn, H., De Meyer, S. F., & Vanhoorelbeke, K. (2017). Long-term prevention of congenital thrombotic thrombocytopenic purpura in ADAMTS13 knockout mice by sleeping beauty transposon-mediated gene therapy. *Arterioscler. Thromb. Vasc. Biol.*, *37*(5), 836–844.
- Versteeg, H. H., Heemskerk, J. W. M., Levi, M., & Reitsma, P. H. (2013). New Fundamentals in Hemostasis. *Physiol. Rev.*, *93*(1), 327–358.

- Yang, S., Jin, M., Lin, S., Cataland, S., & Wu, H. (2011). ADAMTS13 activity and antigen during therapy and follow-up of patients with idiopathic thrombotic thrombocytopenic purpura: correlation with clinical outcome. *Haematologica*, 96(10), 1521–1527.
- Zander, C. B., Cao, W., & Zheng, X. L. (2015). ADAMTS13 and von Willebrand factor interactions. *Curr. Opin. Hematol.*, 22(5), 452–459.
- Zheng, X., Chung, D., Takayama, T. K., Majerus, E. M., Sadler, J. E., & Fujikawa, K. (2001). Structure of von Willebrand Factor-cleaving Protease (ADAMTS13), a Metalloprotease Involved in Thrombotic Thrombocytopenic Purpura. *J. Biol. Chem.*, 276(44), 41059–41063.
- Zheng, X. L. (2013). Structure-function and regulation of ADAMTS-13 protease. *J. Thromb. Haemost.*, 11, 11–23.
- Zheng, X. L. (2015). ADAMTS13 and von Willebrand Factor in Thrombotic Thrombocytopenic Purpura. *Annu. Rev. Med.*, 66(1), 211–225.
- Zhou, Y., Eng, E. T., Zhu, J., Lu, C., Walz, T., & Springer, T. A. (2012). Sequence and structure relationships within von Willebrand factor. *Blood*, 120(2), 449–458.

# Addendum I

## Risk Analysis

The laboratory for Thrombosis Research at the KU Leuven Kulak is a laboratory with containment level L1. Experiments conducted during this thesis involved several risks. Precautions were taken regarding the use and exposure to hazardous substances, as well as the use of biological samples which have the potential to transmit infectious diseases.

To minimize the possible threats, a lab coat was worn at all times during the execution of the experiments and protective gloves were worn when working with blood products and/or irritating or potentially carcinogenic products such as OPD (E4), H<sub>2</sub>O<sub>2</sub> (E4), H<sub>2</sub>SO<sub>4</sub> (E4), acetic acid (E3) and NaOH (E3). GelGreen, used for nucleic acid gel staining, is noncytotoxic and nonmutagenic, however wearing gloves when working with this product is recommended. When working with kits, there was always acted in accordance with risk and safety phrases provided by the manufacturer. At the end of each experiment, waste was collected in the appropriate biological or chemical waste bins.

During this thesis, ear biopsies were taken from mice that were sedated with isoflurane (E3) in a sufficiently ventilated room, in accordance with protocols approved by the Institutional Animal Care and Use Committee of KU Leuven (Belgium). The mice were handled with respect and care as the welfare of the mice were central in performing this experiment. Individuals working with mice are obligated to be vaccinated for tetanus, to reduce the risk of infection when a biting or scratching accidents would occur. A special lab coat was worn at all times in the animalium (A1). The biopsies were performed under a fume hood and gloves were worn. Afterwards, hands were washed thoroughly. These general safety rules help to protect against bite- and scratch wound, as well as the development of allergies.

(All information emanates from the database hazardous materials and labels of the KU Leuven or the safety data sheets made available by the manufacturers.)

# Addendum II

## Product information

Table All.1. Product information of all products mentioned in “Part II Materials & Methods”.

Product	Manufacturer/Supplier	Cat. Number
Monoclonal murine anti-HisG antibody	Invitrogen	R940-25
96-well microtiter plate	Greiner	655092
Tween20 (Polysorbate 20)	Acros Organics	233360010
Dried milk powder	Carl Roth	T145.3
Polyclonal goat anti-HSV antibodies conjugated to HRP	Bethyl Laboratories	A190-136P
H <sub>2</sub> SO <sub>4</sub>	Acros Organics	124640010
FLUOstar Omega microplate reader	BMG Labtech	N/A
HRP-labelled streptavidin	Roche	11089153001
FLUOstar OPTIMA microplate reader	BMG Labtech	N/A
Polyclonal goat anti-human IgG (Fc specific) antibodies conjugated to HRP	Sigma	A0170
In-Fusion® HD Cloning Kit	Takara Bio	639650
<i>Agel</i>	New England Biolabs	R0552S
NucleoSpin Gel and PCR Clean-up kit	Macherey-Nagel	740609
<i>BstBI</i>	New England Biolabs	R0519S
Phusion® High-Fidelity DNA Polymerase	New England Biolabs	M0530
1 kilobase (kb) ladder	New England Biolabs	N3232
Bromophenol blue	Acros Organics	403140050
Sucrose	Acros Organics	220900010
NovaBlue Singles™ Competent Cells	Merck millipore	70181-3
Super Optimal broth with Catabolite repression medium	Invitrogen	15544-034
Ampicillin	Roche	10835269001
LB Broth with agar (Miller)	Sigma-Aldrich	L3147
QIAprep Spin Miniprep Kit	Qiagen	27104
Luria Broth Base (Miller's LB Broth Base)	Invitrogen	12795027
The Platinum™ SuperFi™ DNA Polymerase	Invitrogen	12351250
C2C12 cells	ATCC	CRL-1772
Dulbecco's Modified Eagle Medium	Gibco	11965084
Fetal bovine serum	Gibco	10270106
X-tremeGENE™ HP DNA Transfection Reagent	Roche	6366244001

Polyclonal HRP-labelled goat anti-rabbit IgG antibodies	Jackson ImmunoResearch	111-035-144
EndoFree Plasmid Mega Kit	Qiagen	12381
Ethanol	VWR	20820296
Rag1 KO mice	The Jackson Laboratory	002216
Platinum™ Taq DNA Polymerase	Invitrogen	10966018
Heparin ("Part III Results") 100 U/mL	LEO Pharma	N/A

---

# Addendum III

## Buffer compositions

Table AIII.1. Composition 50 mM carbonate/bicarbonate coating buffer (1 L) (pH = 9.6).

Product	Supplier	Cat. Number
50 mM Na <sub>2</sub> CO <sub>3</sub>	Merck	0088534
50mM NaHCO <sub>3</sub>	Acros Organics	217120025

Table AIII.2. Composition PBS\* (1 L) (pH = 6.5).

Product	Supplier	Cat. Number
8 g NaCl	Carl Roth	9265.2
0.2 g KCl	Acros Organics	196770010
1.15 g Na <sub>2</sub> HPO <sub>4</sub> ·2H <sub>2</sub> O	Sigma	71643
0.2 g KH <sub>2</sub> PO <sub>4</sub>	Acros Organics	205920025

Table AIII.3. Composition of HBS buffer (pH = 7.4).

Product	Supplier	Cat. Number
50 mM HEPES	Carl Roth	6763.3
5 mM CaCl <sub>2</sub> ·2H <sub>2</sub> O	Sigma	C3881-500G
1 μM ZnCl <sub>2</sub>	Sigma	208086-100G
0.15 M NaCl	Carl Roth	9265.2

Table AIII.4. Composition of Bis-Tris buffer (pH = 6.0).

Product	Supplier	Cat. Number
5 mM Bis-Tris	Acros Organics	327721000
25 mM CaCl <sub>2</sub> ·2H <sub>2</sub> O	Sigma	C3881-500G
0.005% Tween20	Acros Organics	233360010

**Table AIII.5. Composition of 5 mM acetate buffer (pH = 5.5).**

<b>Product</b>	<b>Supplier</b>	<b>Cat. Number</b>
4.5 mM Sodium Acetate	Acros Organics	217110025
0.5 mM Acetic Acid	Acros Organics	222140025
5 mM MgCl <sub>2</sub>	Acros Organics	413415000

**Table AIII.6. Composition of the NaOH solution (HotSHOT method) (pH = 12.0).**

<b>Product</b>	<b>Supplier</b>	<b>Cat. Number</b>
25 mM NaOH	Fisher Scientific	S/4800/60
0.2 mM Na <sub>2</sub> EDTA	Fisher Bioreagents	BP120-500

**Table AIII.7. Composition of the Tris solution (HotSHOT method) (pH = 5\*).**

<b>Product</b>	<b>Supplier</b>	<b>Cat. Number</b>
40 mM Tris	Sigma	252859
*Note: Adjust pH to pH = 5 with HCl (37%)	Acros Organics	124630010

**LABORATORY FOR THROMBOSIS RESEARCH**

E. Sabbelaan 53  
8500 KORTRIJK, BELGIUM  
tel. +32 56 24 60 61  
karen.vanhoorelbeke@kuleuven.be  
www.kuleuven.be

